Science of the Total Environment 762 (2021) 143961

Contents lists available at ScienceDirect

Science of the Total Environment

journal homepage: www.elsevier.com/locate/scitotenv

Characterization of marine microbial communities around an Arctic seabed hydrocarbon seep at Scott Inlet, Baffin Bay

Margaret A. Cramm [a,*], Bárbara de Moura Neves [b], Cara C.M. Manning [c,1], Thomas B.P. Oldenburg [d], Philippe Archambault [e], Anirban Chakraborty [a], Annie Cyr-Parent [f], Evan N. Edinger [g], Aprami Jaggi [d], Andrew Mort [h], Philippe Tortell [c], Casey R.J. Hubert [a]

[a] Geomicrobiology Group, Department of Biological Sciences, University of Calgary, 2500 University Dr NW, Calgary, Alberta T2N 1N4, Canada
[b] Fisheries and Oceans Canada, Ecological Sciences Section, 80 East White Hills Road, P.O. Box 5667, St. John's, Newfoundland A1C 5X1, Canada
[c] Department of Earth, Ocean and Atmospheric Sciences, University of British Columbia, Vancouver, BC V6T 1Z4, Canada
[d] Department of Geoscience, University of Calgary, 2500 University Dr NW, Calgary, Alberta T2N 1N4, Canada
[e] ArcticNet, Québec Océan, Takuvik Département de Biologie, Université Laval, Québec G1V 0A6, Canada
[f] Department of Economic Development and Transportation, Government of Nunavut, Building 1104A, Inuksugait Plaza, PO Box 1000, Station 1500, Iqaluit, NU X0A 0H0, Canada
[g] Memorial University of Newfoundland, 230 Elizabeth Avenue, St. John's, Newfoundland A1C 5S7, Canada
[h] Natural Resources Canada, 3303 33 Street NW, Calgary, Alberta T2L 2A7, Canada

HIGHLIGHTS

- Methane and liquid hydrocarbons are seeping from the seafloor at Scott Inlet.
- Cold seep benthic megafauna are typical of Arctic marine sediments.
- Soft corals incorporate hydrocarbons into biomass.
- High methane in bottom water drops to background levels in upper water column.
- Pelagic methanotrophs persist in bottom water down current from the cold seep.

GRAPHICAL ABSTRACT

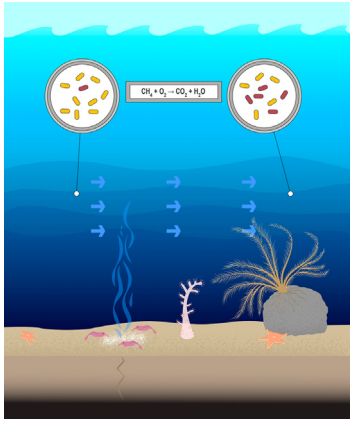

ARTICLE INFO

Article history:
Received 5 September 2020
Received in revised form 13 November 2020
Accepted 15 November 2020
Available online 7 December 2020

Editor: Frederic Coulon

Keywords:
Arctic hydrocarbon seep
Methane
Microbial communities

ABSTRACT

Seabed hydrocarbon seeps present natural laboratories for investigating responses of marine ecosystems to petroleum input. A hydrocarbon seep near Scott Inlet, Baffin Bay, was visited for in situ observations and sampling in the summer of 2018. Video evidence of an active hydrocarbon seep was confirmed by methane and hydrocarbon analysis of the overlying water column, which is 260 m at this site. Elevated methane concentrations in bottom water above and down current from the seep decreased to background seawater levels in the mid-water column >150 m above the seafloor. Seafloor microbial mats morphologically resembling sulfide-oxidizing bacteria surrounded areas of bubble ebullition. Calcareous tube worms, brittle stars, shrimp, sponges, sea stars, sea anemones, sea urchins, small fish and soft corals were observed near the seep, with soft corals showing evidence for hydrocarbon incorporation. Sediment microbial communities included putative methane-oxidizing *Methyloprofundus*, sulfate-reducing *Desulfobulbaceae* and sulfide-oxidizing *Sulfurovum*. A metabolic gene diagnostic for aerobic methanotrophs (*pmoA*) was detected in the sediment and bottom water above the seep

* Corresponding author at: Queen Mary University of London, Mile End Rd, Bethnal Green, London E1 4NS, UK.
E-mail address: m.a.cramm@qmul.ac.uk, (M.A. Cramm).
[1] Plymouth Marine Laboratory, Prospect Place, Plymouth, UK, PL1 3DH.

https://doi.org/10.1016/j.scitotenv.2020.143961

Methanotrophs
Benthic megafauna

epicentre and up to 5 km away. Both 16S rRNA gene and *pmoA* amplicon sequencing revealed that pelagic microbial communities oriented along the geologic basement rise associated with methane seepage (running SW to NE) differed from communities in off-axis water up to 5 km away. Relative abundances of aerobic methanotrophs and putative hydrocarbon-degrading bacteria were elevated in the bottom water down current from the seep. Detection of bacterial clades typically associated with hydrocarbon and methane oxidation highlights the importance of Arctic marine microbial communities in mitigating hydrocarbon emissions from natural geologic sources.

1. Introduction

Methane (CH_4) is a potent greenhouse gas with a radiative global warming potential 32 times that of carbon dioxide (CO_2) over a 100-year horizon (Etminan et al., 2016). Identifying sources and sinks of methane and assessing its flux into the atmosphere is a priority for understanding climate change. This is particularly pressing in polar regions where climate change is occurring faster than at lower latitudes (Serreze and Barry, 2011). In the Arctic, methane is released from melting permafrost, wetlands, and marine environments including methane emissions from cold seeps in the seabed (Elder et al., 2020; Ferré et al., 2020; Parmentier et al., 2013; Shakhova et al., 2010; Thornton and Crill, 2015). At cold seeps methane and other hydrocarbons originating in the subsurface can escape into the overlying water column. These features form when pressurized fluids in the subsurface migrate up toward the seabed through fissures and faults, or other areas of increased permeability. Unlike hydrothermal vents and mud volcanoes, which also release methane and subsurface fluids, cold seeps exhibit lower rates of fluid flow and ambient temperatures close to that of the surrounding seabed (Suess, 2014, 2018), which is near 0°C in the Arctic Ocean.

Cold seeps are hotspots of biological activity on the seafloor where chemical gradients caused by seeping methane and other hydrocarbons fuel microbial communities that in turn support higher trophic levels via symbioses and predation (Demopoulos et al., 2018; Levin et al., 2016). Methane-oxidizing microorganisms (methanotrophs) use methane for carbon assimilation and energy by converting it to biomass and CO_2, thereby mitigating the warming potential noted above (Crespo-Medina et al., 2014; Kessler et al., 2011; Leonte et al., 2017). Microbial mats at cold seeps host diverse populations of methane- and sulfide-oxidizing bacteria (Crépeau et al., 2011). In deeper anoxic sediments, populations of anaerobic methane-oxidizing archaea (ANME) associated with sulfate-reducing bacteria (SRB) attenuate the amount of methane reaching the seafloor and water column (Boetius and Wenzhöfer, 2013) . Methane that migrates past these consortia may still be oxidized by aerobic methane-oxidizing bacteria in the water column, mitigating its release into the atmosphere (Reeburgh, 2007). Indeed, the combined action of anaerobic and aerobic methane biofilters can result in the complete oxidation of methane escaping the seafloor, limiting greenhouse gas emissions at these sites (Boetius and Wenzhöfer, 2013; Reeburgh, 2007).

Benthic organisms living in or on the seafloor can benefit from symbiotic or predatory relationships with methane-seep microbial communities (Seabrook et al., 2019; Thurber et al., 2013). Seeps can create an "oasis-effect" providing heterogenous geologic substrates, such as the presence of carbonate outcrops that allow for the attachment of sessile organisms that may provide shelter for other organisms (Vanreusel et al., 2009; Webb et al., 2009) . Furthermore, chemosynthesis-driven nutrition provision pervading both the seafloor and water column contribute to seeps being biological hotspots (Åström et al., 2018; Carney, 1994; Levin et al., 2016). Corals, sponges, bivalves, tube worms, and shrimp are among the benthic guilds that can derive energetic benefits from methanotrophs and other seep-associated microbial populations through symbiotic relationships or microbial grazing (Hovland and Risk, 2003; Niemann et al., 2013; Thurber et al., 2010, 2013; Zbinden et al., 2008). Predatory species such as crabs, fish, sea stars, and octopuses benefit, in turn, by feeding on the lower trophic levels at the seep, such that methanotrophs and other chemosynthetic microbes form the base of a diverse marine food web in these settings (Levin et al., 2016; MacAvoy et al., 2002; Seabrook et al., 2019; Voight, 2000).

The Scott Inlet cold seep is located in the Canadian Arctic ~40 km east of Scott Inlet in west Baffin Bay (71.37812 N, −70.07452 W; 260 mbsl; Fig. 1A). The Geological Survey of Canada first published reports of this seep in 1977 (Loncarevic and Falconer, 1977) and it has since then been the subject of observations and sample collections involving the use of ships, remote sensing aircraft and submersible vehicles (e.g. Grant et al., 1986; Maclean et al., 1981; Punshon et al., 2019). Previous studies have focused on the marine geology of this site (Levy and MacLean, 1980; Maclean et al., 1981) noting microbial mats and local benthic megafauna (Grant et al., 1986; Levy and Lee, 1988) , but exploration of the connection between this seep and local biota has yet to be reported. Scott Inlet has been identified by the Government of Canada's Department of Fisheries and Oceans (DFO) as an Ecologically and Biologically Significant Area (EBSA) on account of this hydrocarbon seep (DFO, 2015) . The area is relevant to seabirds (Latour et al., 2008; Mallory and Fontaine, 2004) , Greenland Shark including juveniles (Devine et al., 2018; Hussey et al., 2015) , and marine mammals including the Baffin Bay Narwhal population that use Scott Inlet as a nursery (Marcoux et al., 2017) .

In 2018, we returned to Scott Inlet with a remotely operated vehicle (ROV) and Rosette water column sampler to conduct an interdisciplinary study of its microbiology and benthic ecology. The aim of this study is to characterize the benthic biota and microbial community influenced by hydrocarbon seepage. Latitude has been shown to influence the structure of microbial communities at methane seeps (Seabrook et al., 2018). Here we present extensive biological characterization and suggest ways in which the seep communities contribute to methane cycling in the Arctic.

2. Methods

2.1. Seep identification and sampling at Scott Inlet

The location of the seep on the seabed was first determined using a submersible vehicle in 1985 (Grant et al., 1986). The seep sits at a depth of 260 m below sea level (mbsl) and is oriented along a geologic basement rise on the south-eastern flank of Scott Trough (Fig. 1B). Vertical relief is due to Pleistocene glacial scouring and the presence of a structural high, interpreted as Precambrian, on the south-eastern flank of the seabed trough. This feature is thought to be partially responsible for the focusing of deep fluid expulsion along *syn*-rift faults reactivated during the Eocene Eurekan Orogeny (Blasco et al., 2010; Maclean et al., 1981). Seeping fluids reaching the seabed contain hydrocarbons generated from an organic-rich source rock of uncertain identity. The dominant current flows from Northwest to Southeast.

The Canadian research icebreaker CCGS *Amundsen* visited Scott Inlet on August 12 and 13, 2018. Methane seeps were identified via bubble ebullition and microbial mats observed on live video obtained using a Super Mohawk II remotely operated vehicle (ROV). The methane seep identified by the ROV was at 71.37812 N, −70.07452 W (Table S1),

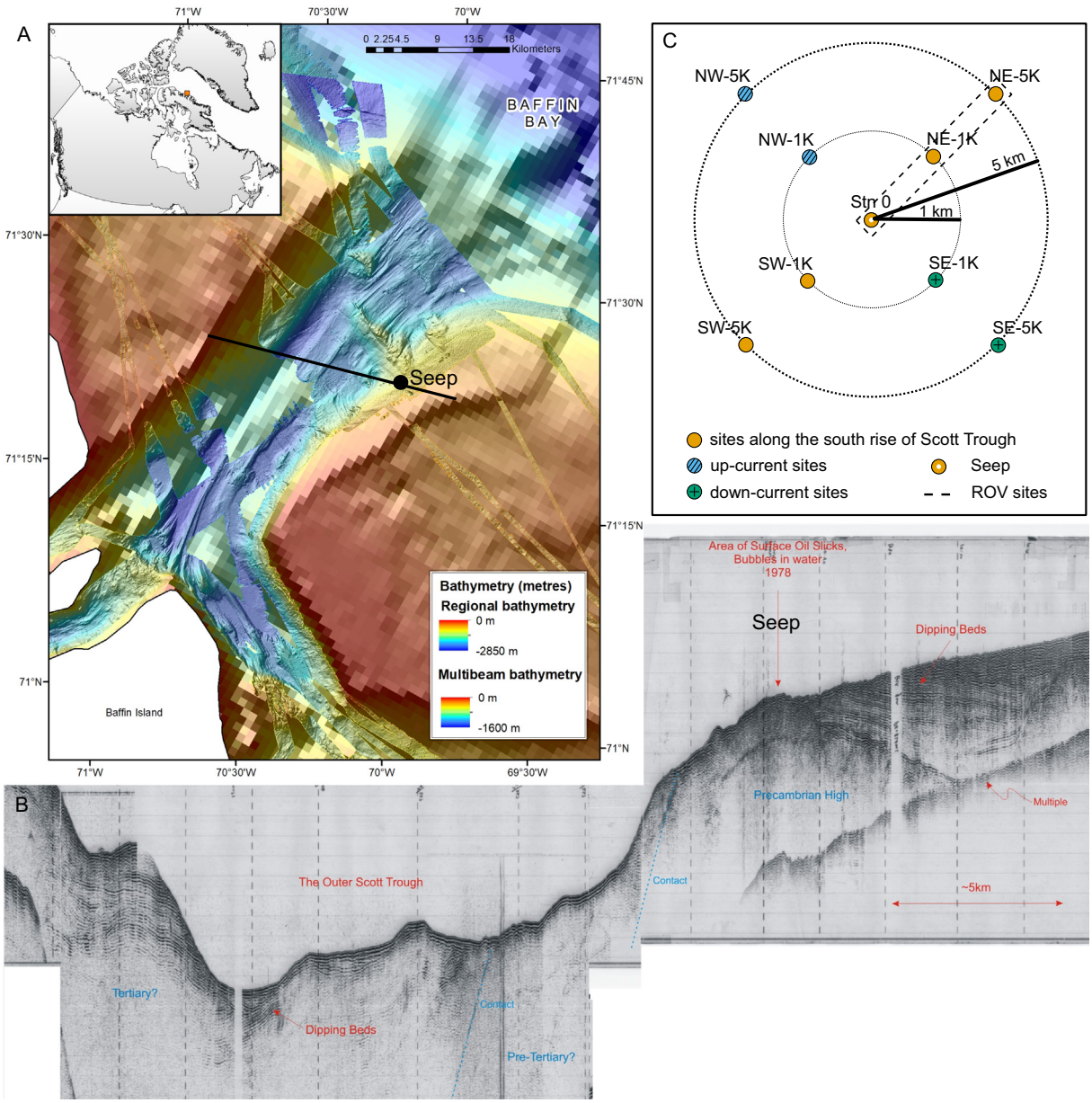

Fig. 1. Scott Inlet, Baffin Bay. The seep denoted as Stn0 in this study (black dot in panel A) lies on the southern rise of Scott Trough. (A) Multibeam data of the regional bathymethry of Scott Trough (courtesy of ArcticNet). Background regional bathymetry was generated from an unpublished Canadian Hydrographic Service database (courtesy of the Geological Survey of Canada). Multibeam data resolution is 25 m and 1000 m. (B) Seismic profile across Scott Trough (cf. black line in panel A) obtained from a 1978 airgun seismic record (CCGS *Hudson* 780290). The profile is axial to the Scott Trough Sub-Basin described in detail elsewhere (Harrison et al., 2011). This image is modified from Blasco et al. (2010) and is published here under the Open Government Licence – Canada, version 2.0 (https://open.canada.ca/en/open-government-licence-canada). (C) Sampling design for the exploration of Scott Inlet, with orange dots identifying sampling sites (SW-5K, SW-1K, Stn0, NE-1K, NE-5K) that lie along the south rise of Scott Tough. Bubble ebullition was observed at Stn0. Blue dots identify sampling sites up current from the seep, and green dots identify sampling sites down current from the seep. The dominant surface current runs NW to SE.

consistent with previous expeditions (e.g. Mort et al., 2013) , and is referred to below as Station 0 (Stn0). Surface oil slicks were observed on September 2 and 3, 2018 during a follow-up expedition onboard the RV *Nuliajuk* (71.402087 N, −70.141945 W).

2.2. Video and photograph collection

Video footage was collected at Stn0 and sites 1 km (NE-1K) and 5 km (NE-5K) away from Stn0 in the NE direction (Fig. 1C). These sites are situated along the geologic basement rise of Scott Trough, the feature on which the seep lies. Video and photographic footage of the seafloor was obtained using an ROV fitted with a forward-looking HD camera (1Cam Alpha, SubC Imaging, 24. 1 megapixels), and a pair of lasers situated 6 cm apart for size estimation. Photos of a surface water oil slick were taken from the RV *Nuliajuk* using a digital camera.

2.3. Water and sediment sampling

Water and sediment were sampled according to the sampling design shown in Fig. 1C and station details shown in Table 1. Water was collected for methane measurements, hydrocarbon analysis, and microbiological analyses. Water sampling was performed with a CTD-Rosette equipped with 24 Niskin bottles each with a 12 L capacity, that were deployed at several depths from surface seawater down to 7 m above the seafloor. Replicates were sampled from a given water depth by collecting water from separate Niskin bottles deployed at that depth.

Table 1
Sampling stations. Additional details are found in Table S1.

Station	Latitude	Longitude	Water depth (m)	Analysis
NW-5K	71.40855	−70.17774	557	CH_4, microbiology
NW-1K	71.38466	−70.09111	312	CH_4, microbiology
NE-5K	71.40957	−69.97310	266	CH_4, microbiology, megafauna, oil
NE-1K	71.38654	−70.05215	254	CH_4, microbiology, megafauna, oil
Stn0 t1	71.37635	−70.07686	260	CH_4, microbiology
Stn0 t2	71.37965	−70.06951	265	CH_4, microbiology, megafauna, oil
Stn0 t3	71.37876	−70.07145	264	CH_4, microbiology
Stn0 t4	71.37845	−70.07475	265	CH_4, microbiology
Stn0 t5	71.37711	−70.07255	262	microbiology
SW-1K	71.37226	−70.09275	251	CH_4, microbiology
SW-5K	71.34725	−70.17225	226	CH_4, microbiology
SE-1K	71.37283	−70.04810	215	CH_4, microbiology
SE-5K	71.35005	−69.96353	216	CH_4, microbiology

Stn0 was sampled five times (t1-t5) over 24 h.

Detailed sample collection information, including sampling depths for water collected for different analyses, are listed in Table S1.

Duplicate water samples for dissolved methane analysis were performed on bottom water collected within 7 m of the seafloor at Stn0 as well as at the NW, NE, and SE stations (Fig. 1C) (methane was not measured at the SW stations). Additional water samples at Stn0 were also collected at the sea surface (≤2 m) and at 10, 30, 50, 100, 150 and 200 mbsl (Table S1). Water samples were transferred from Niskin bottles to 60 mL glass serum vials using silicon tubing. Glass vials were overfilled avoiding bubble contamination and headspace, and immediately preserved with 50 μL of saturated mercuric chloride solution before crimp sealing with chlorobutyl rubber stoppers. Preserved samples were stored at room temperature in the dark until analysis.

Water samples (4 L) were collected at the surface (≤2 m) and bottom water at Stn0, NE-1K and NE-5K to measure dissolved organic matter (DOM) composition. A mid-water column sample at 120 mbsl was also collected at Stn0 for DOM analysis. Immediately following collection, water samples were pumped into pre-cleaned amber glass bottles. After filtration through 0.45 μm glass fiber filters and 0.2 μm membrane filters (Whatman) filtrates were acidified to pH 2 with HCl and extracted with methanol via solid phase extraction (SPE) as described by Dittmar et al. (2008), with styrene-divinylbenzene polymer sorbent (Agilent Bond Elut PPL, 5 g).

Water for microbial analyses (3 L) was collected from the bottom water at every site (Fig. 1C) and from surface water (≤2 m) at Stn0. Five bottom water samples were collected at Stn0 over a 24-h period to assess short-term temporal variability (Table S1). Niskin bottles were emptied via silicon tubing into plastic carboys (both were rinsed twice with water from the same sample before filling the carboy). Water (3 L) was passed through 2 μm pore size, 47-mm diameter sterile filters (PALL) immediately upon collection, and filters were stored at −80°C.

Sediment and benthic invertebrates were sampled at sites Stn0, NE-1K and NE-5K using spatulas fitted to the arms of the ROV. Sediment (~300 mL) was sampled into a container stored inside the ROV sampling skid and was kept separate from the benthic invertebrate samples. Aliquots (~1 mL) of the sediment were immediately frozen at −80°C after the dives. Water that entered the container during ROV sediment collection (referred to as ROV water below) was also collected after the dives by decanting it from the container in the sampling skid (~1 L). When the ROV was stationary on the bottom, the sampling skid at its base was located <20 cm from the seafloor, thus the ROV water that was collected is most likely bottom water from this depth. ROV water was passed through 2 μm pore size sterile filters (PALL) immediately upon collection, and filters were stored at −80°C.

2.4. Video survey of benthic megafauna and microbial mats

A qualitative assessment of benthic megafauna diversity at Scott Inlet was performed through analysis of the ROV video footage. Dive plans prioritized the identification of hydrocarbon seep indicators (e.g. microbial mats and bubble ebullition from the seafloor), sediment sampling, and collection of invertebrates. Since video surveys were not specifically designed for a biodiversity study, video analyses for megafauna benthic diversity were descriptive and non-quantitative.

Separate ROV dives took place at sites Stn0, NE-1K and NE-5K. Additionally, the ROV transited in a straight line between NE-1K and Stn0 to survey seep indicators along the geologic basement rise on the southeast flank of Scott Trough. ROV navigation tracks per second were mapped using ArcMap version 10.6.1. Position accuracy for this system at a depth of 250 m is estimated at 0.26–1.3 m. Images were analyzed by photo frames (i.e. snapshots) extracted from the videos using VLC software. To characterize representative benthic megafauna at a general level at each site, video frames were pre-selected based on their location displayed in ArcMap. Field of view width for pre-selected frames was calculated using the distance between laser points using the software ImageJ (Schneider et al., 2012). Standard deviation of the mean field of view width for the pre-selected frames at each site was used to further filter the frames to account for fluctuating distance from the bottom. If the ROV was too far from the seafloor in a pre-selected frame (e.g. seafloor visibility impaired), then the next suitable frame was used for analysis. The field of view widths for analyzed photo frames ranged between 1.5 and 3.4 m for dive 70 (Stn0, $N = 26$ frames), and between 2.4 and 5 m for dive 71 (NE-1K, $N = 49$) and dive 72 (NE-5K, $N = 33$) respectively, for a total of 108 images. Further information about the ROV dives can be found in the Supplementary Information.

Organisms were mostly identified at a general level (e.g. brittle star, crinoid, sea urchin), and are considered tentative since voucher specimens for confirmation were not collected on this expedition. Some organisms commonly seen during the dives such as tubiculous polychaetes (*Nothria* sp.) and the shrimp *Eualus gaimardii* were collected using an Agassiz trawl in the area between ROV dives (within 600 m SW of Stn0), supporting video-based taxonomic identifications.

2.5. Lipid compositional analyses

Two soft coral colonies (*Pseudodrifa* sp. and *Gersemia* sp., both in family Nephtheidae) were subsampled at NE-1K and NE-5K for lipid classification. Colonies were frozen at −80°C immediately following collection and subsampling using pre-cleaned tools. Entire soft coral branches (including polyps and other tissue) were subsampled in duplicate (0.7–1.0 g) before analysis. Lipid extraction took place at the Northwest Atlantic Fisheries Centre (NAFC, St. John's, NL) according to the methods of Folch et al. (1957) and Parrish (1999). Lipid classes were identified and quantified in an Iatroscan (Lipid Lab, Memorial University, St. John's, NL) by comparing peak position and area with the following commonly used standards: n-nonadecane and phenanthrene (hydrocarbon; HC), cholesteryl palmitate (steryl ester; SE), 3-hexadecanone (ketone), tripalmitin (triacylglycerol; TG), palmitic acid (free fatty acid; FFA), 1-hexadecanol (alcohol; ALC), cholesterol (sterol; ST), 1-monopalmitoyl-rac-glycerol (acetone-mobile polar lipid; AMPL), and DL-α-phosphatidylcholine dipalmitoyl (phospholipid; PL). Lipid data are presented as percentage of lipid composition by class.

2.6. Methane measurements

Dissolved methane was measured using an automated purge and trap system coupled to a gas chromatograph–mass spectrometer (Shimadzu GCMS-QP2010) at the University of British Columbia following the methods of Capelle et al. (2015). Calibration curves were prepared using a Praxair certified gas standard (±5% accuracy for CH_4)

mixed with helium to prepare standards of varying concentrations. Air-equilibrated water samples were analyzed as part of every run to verify measurement accuracy. The laboratory has participated in intercalibration exercises for oceanic methane measurements (Wilson et al., 2018).

2.7. Hydrocarbon analysis

Dissolved organic matter (DOM) methanol extracts were analyzed using a 12 T Bruker SolariX Fourier Transform Ion Cyclotron Resonance-Mass Spectrometer (FTICR-MS) using atmospheric pressure photoionization in positive ion mode (APPI-P) and electrospray ionization in negative ion mode (ESI-N) (Oldenburg et al., 2014, 2017). The APPI-P ionization used a krypton lamp at 10.6 eV as the ion source, with a transfer capillary temperature of 400°C, and a nebulizer pressure of 1.0 bar. APPI-P analyses were conducted using a sample diluted at 0.25 mg/mL in methanol:toluene (1:1). The electrospray ionization parameters included a flow rate of 200 μL/h, 4 kV of capillary voltage, and a nebulizer pressure of 1.0 bar. ESI-N sample solutions were 0.25 mg/mL in methanol, doped with 2% ammonium hydroxide.

The extracts were spiked with 10 μL of a standard mixture prior to analysis to assess internal calibration efficiency (Silva et al., 2016). Ions ranging from *m/z* 150 to 1500 were isolated by a linear quadrupole and accumulated over a period of 5–50 ms in the collision cell, prior to their transfer to the ion cyclotron resonance (ICR) cell. Spectra were collected in absorption mode (Kilgour et al., 2013). Two hundred transients of 8 million points in the time domain were collected and summed to improve the experimental signal/noise ratio (SNR). FTICR-MS raw data were processed using the calibration and peak assignment (CaPA v.1; Aphorist Inc.) software package. Peaks with SNR >5 were assigned based on highly accurate m/z measurements and using the stable isotopic pattern (up to the third most intense isotopologues were used), whenever possible. Elemental composition boundaries used in data processing include $^{12}C_{4-95}$, $^{1}H_{0-200}$, $^{16}O_{0-30}$, $^{14}N_{0-8}$, $^{32}S_{0-2}$, $^{23}Na_{0-2}$, $^{15}P_{0-2}$, and $^{35}Cl_{0-2}$ (with suffixes related to atom number of the molecule), and only assignments with error lower than 300 ppb were accepted. Mass spectra were internally calibrated using pseudohomologous series present in each sample. Solvent blanks were analyzed for each mode, and the most prominent peaks detected in blank spectra were omitted from consideration in the sample results. Data visualization used Ragnarök v.1.7 (Aphorist Inc.).

2.8. DNA extraction

DNA was extracted from biomass collected from filters and from sediment samples using the DNeasy PowerWater and DNeasy PowerSoil DNA Isolation Kits (Qiagen), respectively. DNA extraction from filters was performed as per manufacturer's instructions, with DNA eluted in 30 μL nuclease-free water pre-heated to 50°C. DNA was extracted from 0.3 g sediment according to manufacturer's instructions, with DNA eluted in 100 μL nuclease-free water pre-heated to 50°C.

2.9. 16S rRNA gene amplicon sequencing and analysis

Amplification of a 291 bp region of the V4 region of the 16S rRNA gene in water and sediment DNA extracts used primers 515F (Parada et al., 2016) and 806R (Apprill et al., 2015). Prior to amplification, the DNA used as the template in the PCR reaction was adjusted to 5 ng/μL. Triplicate 25 μL PCR reactions were performed for each sample using 12 μL 2× KAPA HiFi Hot Start Ready Mix (KAPA Biosystems), 2.5 μL of each primer (515F and 806R), 6.5 μL nuclease-free water, and 1 μL DNA template. PCR used a touchdown protocol of initial annealing at 95°C for 3 min followed by 10 cycles of denaturation at 95°C (30 s) followed by primer annealing at temperatures dropping from 60°C to 51°C (45 s), then extension at 72°C (1 min). This was followed by an additional 15 cycles with a consistent annealing temperature of 55°C, ending with a 5 min extension at 72°C. Resulting amplicons were pooled and sequenced on a MiSeq Benchtop DNA sequencer according to Dong et al. (2017), resulting in an average library size of 41,436 reads per sample. Libraries generated through PCR amplification and sequencing of DNA extraction negatives (i.e. blanks that did not include a filter or sediment sample), positive control DNA (20 Strain Even Mix Genomic Material, ATCC® MSA-1002TM), and PCR negative control DNA (i.e. PCR without and DNA template) were included for quality control.

Operational taxonomic units (OTUs) were generated using MetaAmp version 2.0 (Dong et al., 2017). Paired-end merging options for the MetaAmp pipeline included a minimum overlap of 100 bp allowing for 1 bp mismatch in the overlap region, an expected error of 1 bp, and allowing up to 2 bp mismatches to the primer sequence. For quality control, 16S rRNA gene amplicons were trimmed to 250 bp. Sequences were clustered into OTUs using a 97% sequence identify threshold. Taxonomy was assigned to representative sequences for each OTU with the UPARSE-OTU algorithm using the SILVA (version 132) database (Pruesse et al., 2012). Diversity analyses were performed in the R software environment version 3.6.2 (R Core Team, 2019) using the workflow VisuaR (Ruff and Hrabe de Angelis, 2019) and custom scripts. Microbial community composition and ordination were performed using 'ampvis2' version 2.5.5 (Andersen et al., 2018). Sequence similarity to reference 16S rRNA gene sequences was identified through BLASTn searching (Zhang et al., 2000) using the refseq_rna database. Statistical analysis of OTU sequence abundances was performed using DESeq2 version 1.24 (Love et al., 2014).

2.10. pmoA gene amplicon sequencing and analysis

The β-subunit of particulate methane monooxygenase is encoded by the *pmoA* gene, which is used as a molecular target for detecting aerobic methanotrophs (Dumont and Murrell, 2005; McDonald et al., 2008). Normalized DNA template (5 ng/μL) was amplified using water column-specific *pmoA* primers wcpmoA189f and wcpmoA661r (Tavormina et al., 2008). Triplicate 25 μL PCR reactions were performed for each sample using 12.5 μL 2× KAPA HiFi Hot Start Ready Mix (KAPA Biosystems), 2.5 μL of each primer, 6.5 μL nuclease-free water, and 1 μL DNA template. PCR used a protocol beginning with an initial denaturation at 94°C for 5 min, followed by 28 cycles of denaturing at 94°C (30 s), annealing at 56°C (45 s), and extension at 72°C (1 min), and ending with extension at 72°C (5 min).

Amplified DNA sequences were prepared for sequencing on a MiSeq Benchtop DNA sequencer according to Dong et al. (2017). This resulted in average *pmoA* library size of 4110 reads per sample, with libraries of <500 reads excluded from further analysis.

Representative sequences for *pmoA* OTUs were generated by MetaAmp version 2.0 (Dong et al., 2017) using an 86% sequence identity threshold, which corresponds to the 97% identity threshold for 16S rRNA genes in Type I Gammaproteobacterial methanotrophs (Wen et al., 2016). Paired-end merging options for *pmoA* sequencing included a minimum overlap of 50 bp allowing for 5 bp mismatches in the overlap region, an expected error of 1 bp, and 2 bp differences to the primer sequence. Amplicons were trimmed to 400 bp. Taxonomy was assigned to the OTU representative sequences using the classify.seqs command in 'mothur' version 1.39.5 (Schloss et al., 2009) and the *pmoA* gene reference database created by Yang et al. (2016) using the "wang" method, a kmer size of 8, and a cut-off bootstrap value of 80% (Dumont et al., 2014). Representative sequences were aligned against a *pmoA* database using 'muscle' version 3.8.31 (Edgar, 2004) and *pmoA* phylogeny was calculated in 'FastTree' version 2.1.9 (Price et al., 2009) using the GTR nucleotide evolution model and visualized in iTOL version 5.5 (Letunic and Bork, 2019).

2.11. DNA sequences

16S rRNA and *pmoA* gene amplicon sequences can be found in the NCBI Sequence Read Archive under the BioProject accession PRJNA632012.

3. Results

3.1. Visual observations of seafloor hydrocarbon seep indicators

White microbial mats visually similar to those typically found in other seep environments (Seabrook et al., 2018; Teske and Carvalho, 2020; Thurber et al., 2020) were observed at Stn0 (Fig. 2A), in the area that was previously identified as a hydrocarbon seep by the Geological Survey of Canada (Grant et al., 1986; Levy, 1978; Levy and MacLean, 1980). Video footage revealed bubbles seeping out of the seafloor in several locations around Stn0 and along a 1 km transect between Stn0 and NE-1K (Fig. S1; Supplementary Video). Microbial mats were also observed in areas where bubble ebullition was not actively observed at the time of video collection. Microbial mats at Stn0 were estimated to be within a ~40 m diameter region. Exposed carbonate crusts at Stn0 and NE-1K were approximately 1–2 cm thick and up to 30 cm long linear dark grey hard features that appeared slightly irregular in form. No epifauna were observed growing on the crusts (Fig. 2F). Two weeks after the ROV survey, a surface water slick was observed in the same area 3.5 km NW of Stn0 (71.402087 N, −70.141945 W; Fig. S2).

3.2. Benthic megafauna video surveys

Photo frames selected for Stn0 captured an area within a 190 m-perimeter polygon where the average water depth was 274 ± 1.0 m. The seabed within this area was dominated by pebbles on a sandy matrix

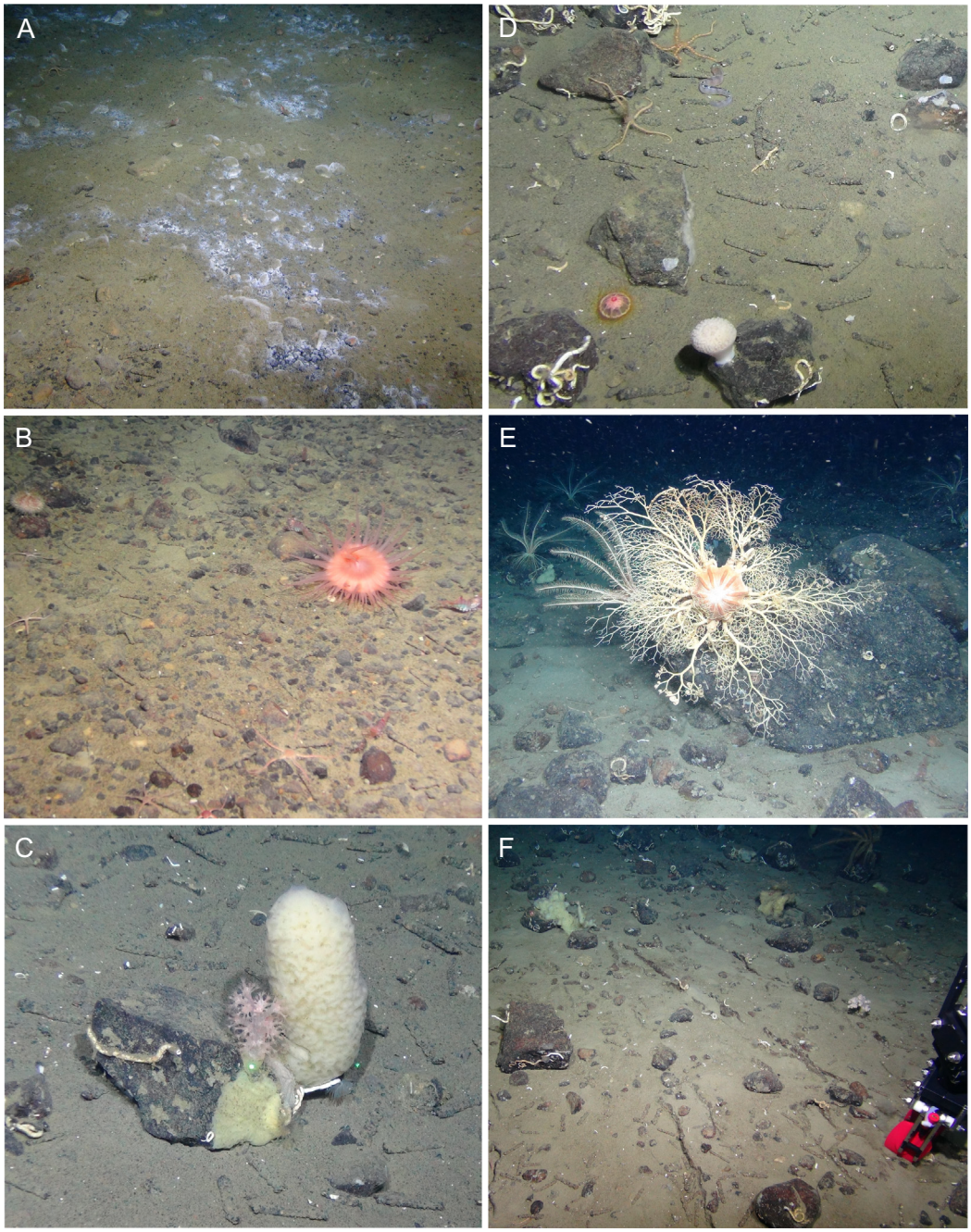

Fig. 2. Scott Inlet seafloor images obtained during dives with the Super Mohawk II Remotely Operated Vehicle (ROV) on August 12 and 13, 2018. Features of particular interest included microbial mats (A), shrimp (*Eualus gaimardii*) urchins and anemones (B), soft corals (Nephtheidae) and sponges (*Mycale*-like) (C), worm tubes (*Nothria* sp.), brittle stars, benthic jellyfish (resembling *Ptychoaastria polaris*), sponges (*Tentorium*-like) and demersal fish (*Gymnelus* sp.) (D), basket stars (*Gorgonocephalus* sp.) and crinoids (E), and carbonate crusts (F).

(69% of frames, Fig. 2A, B). Polygons from sites NE-1K and NE-5K have perimeters 160 m and 193 m, and average water depths of 263 ± 1.4 m and 273 ± 1.3 m, respectively. The bottom at both NE-1K and NE-5K was variable composed of cobbles and boulders, and areas dominated by pebbles (Fig. 2C–F).

Stn0 was characterized by the presence calcareous tube worms (likely *Nothria* sp.; Fig. 2C–F) and brittle stars (usually >10 per field of view; Fig. 2B). Shrimp, small sponges (e.g. *Tentorium*-like), unidentified sea stars, sea anemones, sea urchins, and small fish (e.g. *Gymnelus* sp.) were also observed at this site (Fig. 2B–F). At NE-1K sponges were particularly common in areas dominated by boulders and cobbles, and less abundant in pebble-dominated areas where brittle stars and *Nothria*-like tube worms were more common. Sponges included erect (e.g. *Mycale*-like) and other smaller forms (e.g. *Tentorium*- and *Polymastia*-like). Encrusting worm tubes were also common in areas dominated by cobbles and boulders. Shrimp, sea urchins, soft corals and benthic jellyfish (resembling *Ptychoaastria polaris*) were also observed at this site, whereas less common organisms included sea stars, sea anemones, and small demersal fish (resembling *Gymnelus* sp.) (Fig. 2D). At NE-5K crinoids were the most conspicuous benthic megafauna (>100 individuals in total). Crinoids were not observed in the frames analyzed for the other dives, though sparse distributions were noted ~23 m SE of Stn0 where seep indicators were identified on the initial reconnaissance dive that discovered Stn0. Brittle stars were also common, along with *Nothria*-like tube worms, particularly in areas where pebbles were the dominant substrate type. Sponges (*Mycale*-like) were observed at NE-5K, but they were not as abundant as at NE-1K. Nephtheidae soft corals and the sea star *Leptasterias polaris* were also observed at NE-5K. Less frequently observed organisms included benthic jellyfish, sea anemones, the basket star *Gorgonocephalus* sp. (Fig. 2E), and small demersal fish (Fig. 2D). Overall, Stn0, NE-1K and NE-5K harboured diverse benthic megafauna that were qualitatively similar.

Shrimp (*Eualus gaimardii*) were observed in 85%, 40%, and 27% of the analyzed frames at Stn0, NE-1K, and NE-5K, respectively. A maximum of five individuals per frame were counted at Stn0, which may represent an underestimate due to variable video resolution and distance from the seafloor precluding observation of small individuals. Shrimp were the only epibenthic invertebrates noticed on top of microbial mats, with others such as brittle stars and sea urchins observed between microbial mats. During ROV sediment sampling, shrimp would approach the sampling area, gather around the holes created by removal of the sediment, and actively move their claws in a behaviour possibly indicative of uptake of organic matter suspended during sediment disturbance (see Supplementary Video).

Limited video of the 1 km transect between NE-1K and Stn0 revealed variable bottom types, with cobbles and pebbles as the most common primary substrate. Sponges and encrusting tube worms were abundant in areas where larger substrates (cobbles or boulders) were present in the area surrounding NE-1K, but not further toward Stn0. Overall, brittle stars were the most conspicuous organisms, with worm tubes, small *Tentorium*-like sponges, sea urchins (and skeletons), sea stars, and soft corals also observed.

3.3. Lipid analysis of soft corals collected at NE-1K and NE-5K

Two Nephtheidae coral specimens were collected for lipid analysis to identify the effect of the naturally seeping hydrocarbons on benthic megafauna in the vicinity. The analysis revealed variable lipid class compositions in these soft corals. For *Pseudodrifa* sp. (Fig. 3B) collected 1 km from the seep at NE-1K, hydrocarbons were the main lipid class (33.0 ± 1.7%), followed by Acetone Mobile Polar lipids (23.6 ± 2.8%) (Fig. 3A). This was not observed for *Gersemia* sp. (Fig. 3C) collected 5 km from the seep at NE-5K, which was dominated by steryl esters and wax esters (51.0 ± 1.0%), followed by phospholipids, with hydrocarbons making up 1.7% of the lipid composition (Fig. 3A).

3.4. Dissolved organic matter and hydrocarbons in the water column

Dissolved organic matter (DOM) analysis by FTICR-MS revealed that the compound class distribution of the bottom water samples is dominated by the Ox class group (O1 to O14 with highest abundances for O7 compounds), followed by N1Ox, N2Ox and N3Ox compound class groups, and lowest abundances and variety for N4Ox classes (Fig. 4A). This distribution pattern is typical for seawater. In addition to the DOM, relatively high abundances of hydrocarbons were observed, with the highest levels observed at Stn0. An examination of total hydrocarbon abundances with water depth revealed a decrease with distance from Stn0, with bottom water exhibiting higher concentrations than surface samples (Fig. 4B).

3.5. Dissolved methane in the water column

The concentration of dissolved methane in the bottom water ranged from 4 to 610 nM and was highest at Stn0 and lowest at NW-1K and NW-5K (Fig. 5A). In the NE and SW stations oriented along the southern rise of Scott Trough (Fig. 1C), methane was higher in bottom water of the stations 1 km away from Stn0 (Fig. 5A). Methane samples at Stn0 over a ~24-hour period (Table S1) revealed variability in the bottom water between 9 and 609 nM. Depth profiles of methane taken ~14 h apart at Stn0 (Fig. 5B, C) showed methane concentrations remaining elevated in the bottom 100 m of the water column, above which it was at background levels (near atmospheric equilibrium) observed elsewhere in the Baffin Island shelf seawater (Fenwick et al., 2017; Punshon et al., 2019). Methane profiles at Stn0 are similar to observations made in 2012 at another location in Scott Inlet by Punshon et al. (2019) , who measured 60 nM in the bottom water at Scott Inlet; this is consistent with the spatial and temporal variability in bottom water methane concentration reported here (Fig. 5).

3.6. Microbial community structure

Species richness (OTU count and Chao1 Index) and evenness (Inverse Simpson Index and Shannon Entropy) were lower in the sediment at Stn0 compared to sediment samples collected at NE-1K and NE-5K (Fig. S3A). Putative methane-oxidizing and sulfate-reducing bacteria detected in the sediment and microbial mats include members of the genus *Methyloprofundus*, members of the SEEP-SRB4 *Desulfobulbaceae* family, and several members of the genus *Sulfurovum* within the family *Sulfurovaceae* (Fig. 6B). Many members of these clades were not found 1 km (NE-1K) and 5 km (NE-5K) from the seep at Stn0. Clades of anaerobic methane-oxidizing (ANME) archaea were found only at Stn0 where 4 OTUs had a combined relative abundance of 1.5% (Table 2), with the most abundant OTU being affiliated to ANME2a/b and making up 1.1%. Sequences affiliated to members of *Desulfobacteraceae* were found in higher relative abundance at Stn0 as well as 5 km away from the seep (NE-5K) where no evidence of methane seepage was observed (Table 2).

Overall, microbial signatures considered to be indicators of methane seeps (as defined by Pop Ristova et al. (2015) and Ruff et al. (2015)) were more prevalent in sediment from Stn0 than in sediment 1 km and 5 km away (Table 2). Only three OTUs affiliated to the white mat-forming *Beggiatoaceae* family were detected in the sediment at Stn0 and these only in very low relative abundance (<0.05%), including one affiliated to "*Candidatus* Marithrix", which forms mats very similar in morphology to those seen at Scott Inlet (Teske and Carvalho, 2020). Sequences of putative aerobic methanotrophs as defined by Chistoserdova and Lidstrom (2013), were also more abundant in 16S rRNA gene amplicon libraries for Stn0 sediment (7.8% of the relative sequence abundance) than at NE-1K and NE-5K where they were ≤1% relative sequence abundance (Table 2).

In bottom water (i.e. 7 m above the seafloor) 16S rRNA gene microbial community profiles did not include strong signals for the *Sulfurovaceae*,

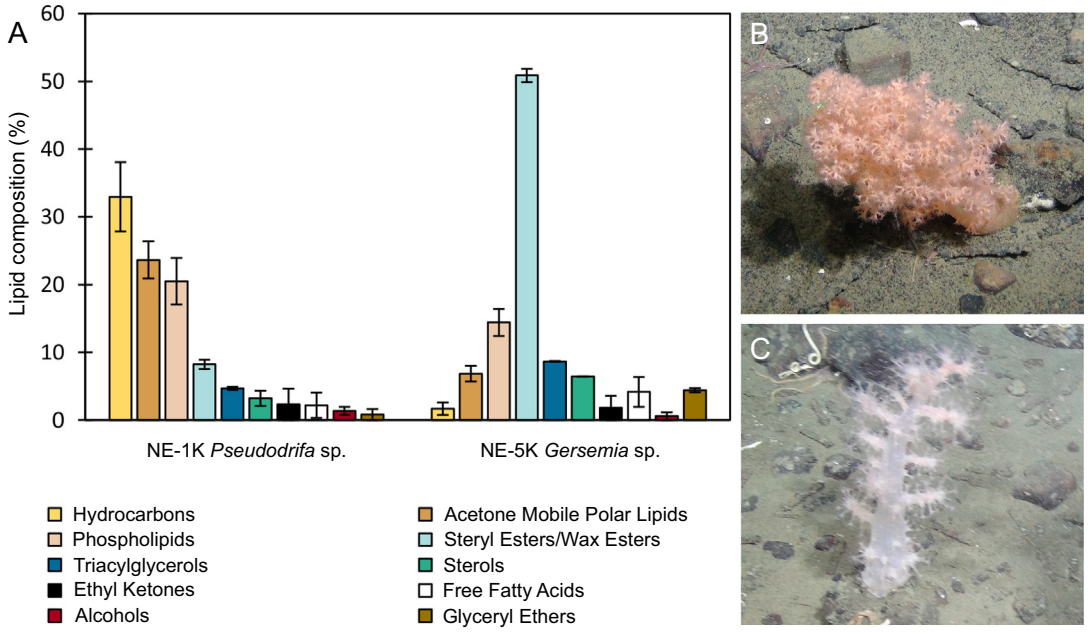

Fig. 3. Average lipid class composition (% of total lipids; A) for soft coral colonies of *Pseudodrifa* sp. sampled at NE-1K (B), and *Gersemia* sp. sampled at NE-5K(C). Error bars represent standard deviation.

Methylomonaceae, *Desulfobulbaceae* and *Thiotrichaceae* groups mentioned above as being prevalent in the surface sediments (Fig. 6A). Comparison of bottom water libraries reveal the microbial communities along the SW-NE oriented Scott Trough (Fig. 1) are more similar than the off-axis (NW-SE) communities (Fig. S4). Considering either axis, microbial communities closer to the seep (i.e. 1 km away from Stn0) were more similar to Stn0 communities than those 5 km from the seep (Fig. S4). All water column communities were dominated by *Nitrosopumilaceae*, SAR11 Clade I, and *Thioglobaceae*. *Flavobacteriaceae* and an unidentified OTU within the *Gammaproteobacteria* (OTU4) make up a larger proportion of the SE communities down current from the seep (Fig. 6A). Richness and evenness were comparable between all bottom water communities with the exception of SE-5K which showed higher evenness and the SE-1K communities which show lower richness (Fig. S3B).

Relative sequence abundance of specific OTUs affiliated to the dominant clades in the bottom water communities highlight these spatial trends. Members of the *Flavobacteriaceae* are in higher relative abundance in the bottom water from Stn0 and SE-1K and SE-5K (Fig. 6A) including *Polaribacter* OTU 14 and *Aurantivirga* OTU 23. The *Colwelliaceae* clade is dominated by two *Colwellia* OTUs, one being in higher relative sequence abundance at Stn0, SE-1K, SE-5K, and SW-5K and the other in higher relative sequence abundance only at SE-1K. Interestingly, OTUs of putative aerobic methanotrophs (cf. Chistoserdova and Lidstrom, 2013) do not exceed 1% relative sequence abundance in any of the bottom water 16S rRNA gene libraries. Nevertheless, patterns at this low relative abundance are still evident, reflecting overall spatial trends described above with putative aerobic methanotrophs more prevalent in bottom waters at and down current (SE direction) from the seep at Stn0 (Fig. 7).

3.7. pmoA gene assessment of methanotrophic microbial communities

To further investigate the occurrence and distribution of methanotrophs, the methane monooxygenase gene, *pmoA*, was amplified and sequenced from sediment and bottom water samples. All *pmoA* OTUs present in >1% relative abundance belong to the *Gammaproteobacteria* (Fig. S5) with the two most abundant OTUs, pmoA1 and pmoA2, together making up >97% of all bottom water libraries (Fig. 8). Both of these OTUs are affiliated with the Deep sea-3 clade, also known as OPU3, within the gammaproteobacterial order *Methylococcales*. The mean relative sequence abundance of pmoA1 was generally much higher than pmoA2, with the exception of the down-current SE-1K and SE-5K bottom waters where pmoA2 was consistently >38% relative sequence abundance (Fig. 8).

Richness of *pmoA* sequences was much higher in the sediment and ROV water, with rarefaction curves demonstrating that these libraries did not capture all *pmoA* diversity present, as opposed to the bottom water samples where it is very likely that *pmoA* diversity was adequately sampled (Fig. S6). Both sediment and ROV water *pmoA* libraries were dominated by OTUs belonging to the Deep sea-1 clade, also within the *Methylococcales* (Fig. S7). *Methyloprofundus* belongs to this clade (Knief, 2015; Tavormina et al., 2015) and it is likely that some Deep sea-1 *pmoA* OTUs correspond to the *Methyloprofundus* OTUs identified by the 16S rRNA gene sequencing. Amplification and sequencing of *pmoA* were unsuccessful in samples of Stn0 surface seawater (15 and 33 sequence reads obtained; Fig. S7), where methane concentrations are very low (Fig. 5B, C) hence these bacteria are expected to be present in much lower abundance.

4. Discussion

4.1. Microbial community structure at Scott Inlet

At Scott Inlet, microbial communities in the sediment and bottom water show a distinct spatial distribution above and around the seep. Methanotrophs are more diverse in the sediment than in the overlying water column. This is congruent with the observations of other studies (Hamdan et al., 2013; Tavormina et al., 2008) that show *pmoA* in sediment and water column populations to be distinctly different and suggest methane-oxidizing bacterial communities in these environments do not establish simply via methanotroph dispersal between the sediment and water column, as suggested in other contexts (Walsh et al., 2016). Several Deep sea-1 *Methylococcales* OTUs were observed in the sediments based on *pmoA* sequencing. These methanotrophs are often found in methane-rich sediments associated with microbial mats or hydrothermal vent fauna, but are rarely detected in the water column except in methane plumes (Li et al., 2014). *Methylococcales* were not detected in the water column at Scott Inlet. In the sediment at the origin

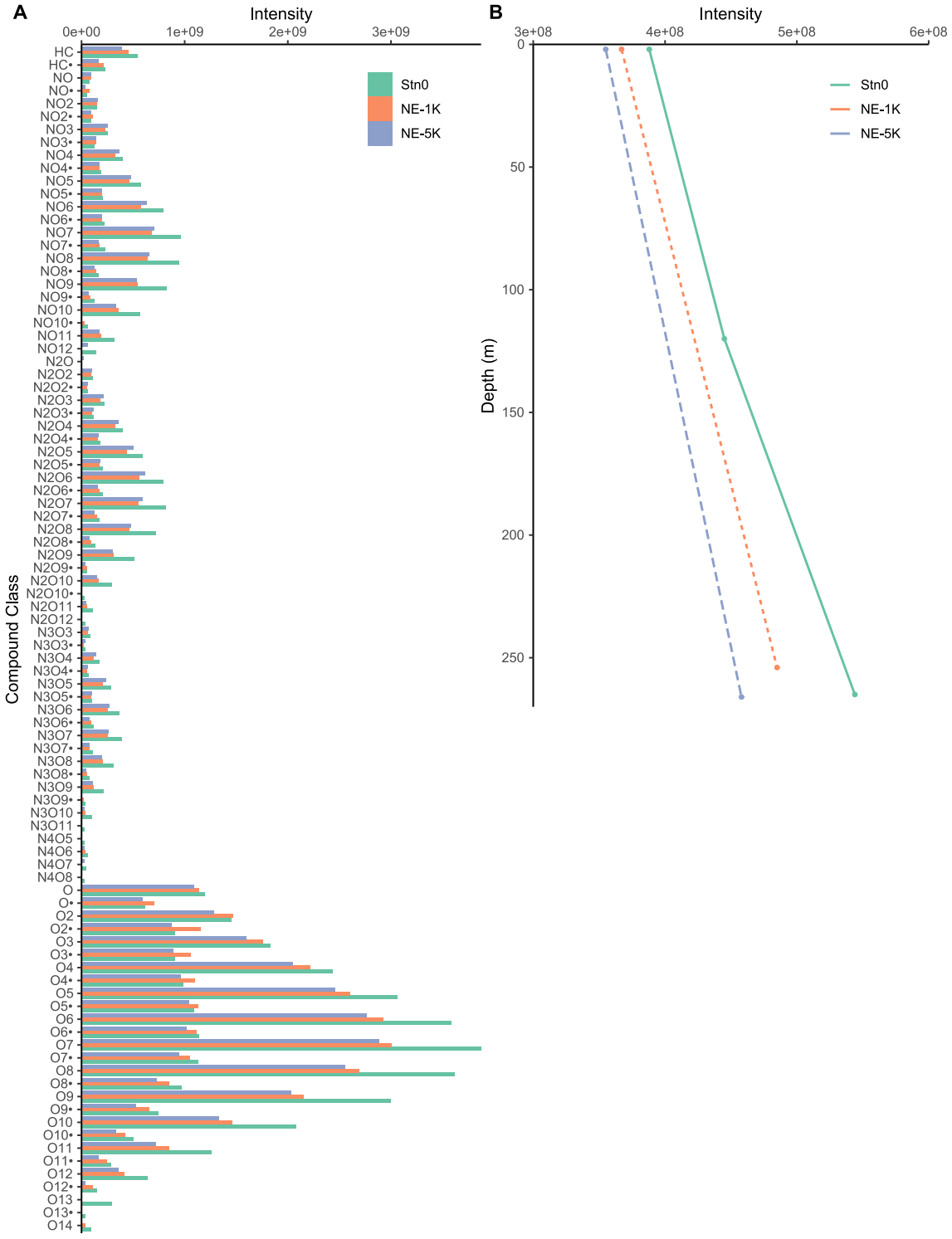

Fig. 4. Compound class distribution of protonated and radical ion species (denoted with a dot •) in the DOM spectra from water samples analyzed by FTICR-MS in APPI-P mode. Spectra from bottom waters at Scott Inlet sites Stn0, NE-1K and NE-5K are compared (A), showing a decrease in relative intensity of the compound class distribution shows with increasing distance from Stn0. Total intensities of dissolved hydrocarbons (protonated) at these sites at different sampling depths (B) reveal that dissolved hydrocarbons decrease with distance from Stn0 and that bottom water contains higher concentrations than surface water.

of the bubbling methane stream, methanotrophs requiring higher methane concentrations may proliferate. As methane emitted from the seabed gets diluted in the water column, pelagic methanotrophs adapted to lower concentrations may be selected. Consistent with this, *pmoA* analysis revealed a predominance of Deep sea-3 *Methylococcales* OTUs in the water column. The Deep sea-3 clade is distributed widely in methane systems and pelagic environments and has similarly been shown to have site-specific distribution in other marine settings (Li et al., 2014; Tavormina et al., 2008). In Scott Inlet bottom water nearly all methanotrophs identified by *pmoA* sequencing belonged to the Deep sea-3 *Methylococcales*.

Different DNA-based analyses suggest that prevailing currents further influence pelagic microbial community structure in relation to methane entering the water column at Stn0. Water currents at Scott Inlet flow

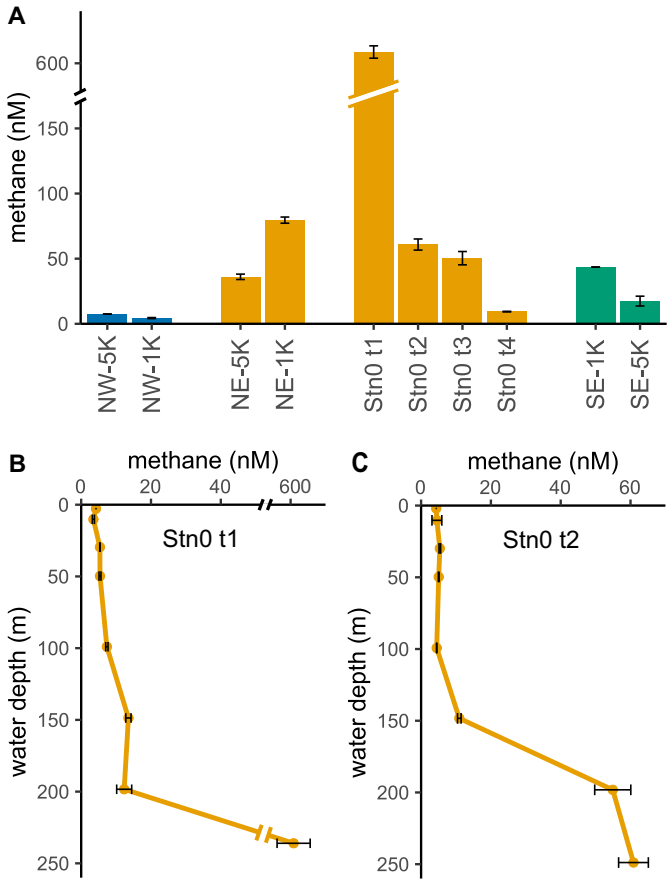

Fig. 5. Water column methane concentration at Scott Inlet. (A) Methane concentration in the bottom water varies with geographic orientation in relation to the seep. Sites up current from Stn0 are shown in blue and those down current from Stn0 are shown in green. Sites situated along the south edge of the Scott Trough rise are shown in orange. Depth profiles of methane concentration at Stn0 determined 14 h apart (Table S1) are shown (B) and (C). Results are reported as the mean of duplicate samples. Background methane concentration in seawater in this region are ~4 nM (Punshon et al., 2019).

NW to SE, perpendicular to the orientation of hydrocarbon seepage along the southern ridge of Scott Trough, which runs SW to NE (Fig. 1). Silyakova et al. (2020) observed the primary mechanisms controlling methane dispersal to be horizontal water movement and eddies near areas of shallow (<120 m) Arctic methane seepage, and suggest that this dispersion influences biological methane oxidation. At Scott Inlet, aerobic methanotrophs and putative hydrocarbon-degrading bacteria were observed in higher relative abundance down current from Stn0. Although these groups exhibited relatively low sequence abundance in 16S rRNA gene libraries, this should not imply that they do not impact local biogeochemistry, including C1 cycling (Bodelier et al., 2013; Jousset et al., 2017; Neufeld et al., 2008). OTUs affiliated to lineages known to include hydrocarbon degraders like *Polaribacter* and *Colwellia* (Mason et al., 2014; Redmond and Valentine, 2012; Tremblay et al., 2019) were detected in higher relative sequence abundance down current from Scott Inlet. Interestingly, among methanotroph OTUs detected in the water column by *pmoA* sequencing, a shift between Deep sea-3 OTUs from pmoA1 to pmoA2 is observed when comparing the bottom water up current (NW) and down current (SE) from Stn0 (Fig. 8). It thus appears that methane-oxidizing bacterial communities persist in this southeastward-moving water column even at low methane concentrations.

Enrichment of methane-oxidizing and hydrocarbon-degrading bacteria at cold seeps may explain the occurrence of these groups in low abundance in the marine environment more generally, e.g. contributing to the occurrence of methanotrophs in pristine ocean systems (van de Kamp et al., 2019) and the ubiquity of methanotrophy in the ocean (Valentine, 2011). Following the 2010 Deepwater Horizon oil spill in the cold deep waters of the Gulf of Mexico, aerobic methanotrophs in the water column oxidized nearly all methane that was released from the sub-sea blowout, preventing its release into the atmosphere (Crespo-Medina et al., 2014; Kessler et al., 2011; Yvon-Lewis et al., 2011). Rare yet ubiquitous marine methanotrophs and hydrocarbon-degrading bacteria in the Canadian Arctic may oxidize methane and other hydrocarbons should pristine Arctic marine environments become exposed to methane and other hydrocarbons by release from decomposing methane hydrates in a warming ocean or the release of hydrocarbons due to offshore oil and gas activity.

4.2. Benthic megafauna at Scott Inlet

Cold seep habitats around the world can host rich benthic communities . Seepage at Scott Inlet supports chemosynthetic microbial communities in the sediment and water column, and the development of microbial mats on the seafloor. Shrimp were the only animal observed directly on the microbial mats and their behaviour at the sampling sites may indicate attraction to sediment resuspension which could occur during ebullition of methane bubbles. Tanner crabs are known to feed on microbial mats at seeps (Seabrook et al., 2019) and snow crabs have been observed grazing on microbial mats at an Arctic cold seep in the western Barents Sea (Sen et al., 2018).

Evidence of a hydrocarbon-fueled food web in this environment was also observed in the lipid composition of Nephtheidae soft corals. A *Pseudodrifa* specimen collected at NE-1K, 1 km away from Stn0 seepage, was dominated by hydrocarbons (33% of total lipid composition), which is high compared to cold-water corals in non-seep environments. For example, in the Flemish Cap area (Northwest Atlantic), hydrocarbons contributed <10% ($N = 5$) of Nephtheidae soft coral lipids and <4% of cold-water corals more generally (Salvo et al., 2018). These lower values are consistent with observations of a *Gersemia* soft coral sampled at 5 km from Stn0 (NE-5K), where the concentration of hydrocarbons in the bottom water was lower (Fig. 4B). A high contribution of hydrocarbons relative to other lipid classes may reflect incorporation of seep-derived fluids during biosynthesis through either direct uptake via feeding or bacterial symbiosis (e.g. Goffredi et al., 2020).

In addition to providing chemosynthetic nutrition, “pavements of carbonates” created through anaerobic microbial activity at some cold seeps can provide substrates for attachment by benthic fauna and thereby contribute to the “biological oasis” effect seen at some seeps (Levin et al., 2016). Primary hard bottom substrate is an important variable to be considered at Scott Inlet, where variable bottom types are present (e.g. gravel, cobbles, boulders) potentially influencing benthic fauna composition (Edinger et al., 2011; Levin et al., 2016; Neves et al., 2014). For instance, areas with high concentration of sponges (NE-5K) feature seafloor dominated by boulders and cobbles. At nearby locations where primary substrate shifted to pebbles, errant organisms such as brittle stars and tube worms were the main fauna observed. Overall, areas where exposed carbonate crusts were observed did not represent hotspots of benthic diversity. They were relatively inconspicuous and did not appear to host novel fauna relative to other sites in the study area. The seafloor substrate at Scott Inlet is already variable, likely due to the presence of ice-rafted debris (Meredyk et al., 2020) , such that hard substrates offered by seep carbonates may not be advantageous to megafauna. While some taxa were spatially restricted (e.g. crinoids, sponges), most were observed throughout the entire study area (e.g. shrimp, tube worms, brittle stars, soft corals, benthic jellyfish) and are typical of other Arctic benthic environments (Bouchard Marmen et al., 2017; Dale et al., 1989; Roy et al., 2014).

Notably absent on the seafloor at Scott Inlet were siboglinid worms and bathymodiolin mussels that are typically observed at seeps (Levin et al., 2016). Water depth is likely a factor controlling the distribution of seep-endemic and symbiont-bearing fauna with these being absent

Fig. 6. Microbial community composition in Scott Inlet bottom water (A), sediment (B), and in both sediment and water collected at Stn0 (C) based on 16S rRNA gene amplicon sequencing. Family-level microbial taxonomy is shown.

near shallower Arctic seep environments, where non-symbiont-bearing heterotrophic fauna are dominant (Åström et al., 2016, 2019; Sahling et al., 2003) . This distribution may be due to increased predation in shallower zones preventing sessile seep-endemic fauna from becoming established (Sahling et al., 2003) , and more photosynthetic input from primary production which reduces the chemosynthetic nutritional advantages of the seep environment (Åström et al., 2019) . Seafloor microbial mats, including sulfide-oxidizing manifestations of hydrocarbon-fueled anaerobic metabolism in seep sediments, were detected but are notably sparse at Scott Inlet. Limited observations of seep-associated benthic communities may also hint at a low methane flux at Scott Inlet that is insufficient for establishing and supporting dense chemosynthetic populations. Bernardino et al. (2012) suggest that fluid flux structures the diversity and abundance of microbial mats and benthic megafauna at seeps. Alternatively, the seep at Scott Inlet may be too young for these communities to have fully developed yet (Levin et al., 2016; Seabrook et al., 2018; Thurber et al., 2020).

Table 2
Relative abundance of seep-associated populations in sediment.

Station	ANME	*Desulfobacteraceae*	Seep indicator clades	Aerobic methanotroph clades
Stn0	1.5%	1.8%	23.0%	7.8%
NE-1K	0%	0.5%	1.9%	1.1%
NE-5K	0%	4.7%	7.6%	0%

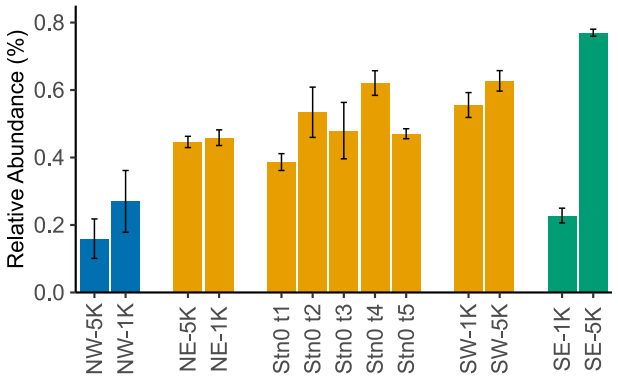

Fig. 7. Relative sequence abundance of bacterial clades affiliated to aerobic methanotrophs (as defined by Chistoserdova and Lidstrom (2013)) in bottom water at Scott Inlet based on 16S rRNA gene amplicon sequencing. All aerobic methanotrophs identified using the 16S rRNA gene amplicon assay were affiliated to *Methylomonaceae*.

5. Conclusion

In the Arctic the impact of climate change is more pronounced than in low latitude regions and warming oceans can be expected to further promote the release of methane from decomposing subsurface hydrates (Ferré et al., 2020) . ROV video footage at Scott Inlet did not reveal dense populations and close associations between bacteria and higher organisms, possibly due to the shallow depth of this hydrocarbon seep, predation and primary production input, or a relatively low flux of hydrocarbon fluids. Methane seepage at Scott Inlet does not represent a notable source of greenhouse gas emissions to the atmosphere due to its attenuation by diverse methanotrophic bacteria in sediments and the overlying water up to 5 km away from the seep. This demonstrates how bacterial populations, even if present in relatively low abundance, can regulate methane flux from the subsurface to the atmosphere. In this way, marine microbial communities can play an important role in mitigating greenhouse gas emissions.

Supplementary data to this article can be found online at https://doi.org/10.1016/j.scitotenv.2020.143961.

CRediT author statement

Margaret A. Cramm: Conceptualization, Formal analysis, Funding acquisition, Investigation, Methodology, Writing – original draft, Visualization; **Bárbara de Moura Neves:** Conceptualization, Formal analysis, Investigation, Methodology, Writing – original draft, Visualization; **Cara C. Manning:** Formal analysis, Writing – original draft; **Thomas B. P. Oldenburg:** Formal analysis, Writing – original draft, Visualization; **Philippe Archambault:** Methodology, Supervision, Writing – review & editing; **Anirban Chakraborty:** Conceptualization, Methodology, Investigation, Writing – review & editing; **Annie Cyr-Parent:** Funding acquisition, Investigation, Project administration; **Evan N. Edinger:** Investigation, Methodology, Writing – review & editing; **Aprami Jaggi:** Investigation, Methodology; **Andrew Mort:** Investigation, Methodology; **Philippe Tortell:** Supervision, Writing – review & editing; **Casey R. J. Hubert:** Funding acquisition, Project administration, Resources, Supervision, Writing – review & editing.

Declaration of competing interest

The authors declare that they have no known competing financial interests or personal relationships that could have appeared to influence the work reported in this paper.

Acknowledgements

We acknowledge funding and support from ArcticNet, Genome Canada and the Government of Alberta for the GENICE project, and the Marine Environment Observation, Prediction, and Response (MEOPAR) Investigator Networking Fund. Ship time funding from NSERC (grant RGPST-515528-2018) and CFI (Major Science Initiatives grant 35560 to Amundsen Science) is also gratefully acknowledged. We would especially like to thank ROV operators Vincent Auger and Peter Lockhart (Canadian Scientific Submersible Facility, CSSF), and Barry Brake (CSSF) and Kandice Piccott for expert ROV technical support. We thank Commandant Claude Lafrance and the crew of the CCGS *Amundsen* for facilitating a successful expedition. Vonda Wareham Hayes is thanked for assistance operating the ROV digital camera, Robert Izett and Katarzyna Polcwiartek are thanked for assistance with water sampling, and Ross McCulloch and Zhiyin Zheng are thanked for assistance with methane measurements. Carmen Li performed Illumina MiSeq sequencing at the University of Calgary, and Jeanette Wells assisted with lipids extraction and analysis at Memorial University. Robbie Bennett provided the regional bathymetry map of Scott Inlet. Elizabeth Cramm created the online graphical abstract. We appreciate valuable discussions with Rhonda Clark, María Bautista, Srijak Bhatnagar, Jianwei Chen, Carmen Li, and Alastair Smith, and are grateful to Rhonda Clark for operational and fieldwork logistical support.

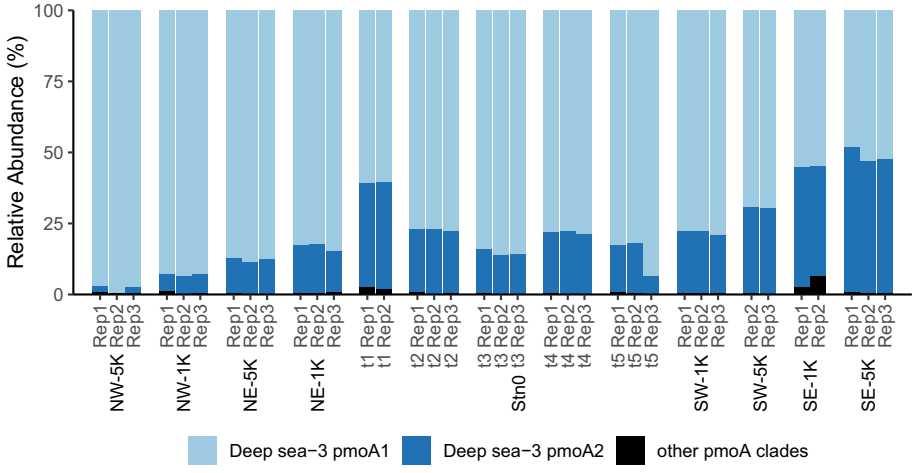

Fig. 8. Relative sequence abundance of *pmoA* OTUs in the bottom water at Scott Inlet. Methanotrophs represented by pmoA2 exhibit a marked increase down current from the seep in the SE-1K and SE-5K bottom water.

References

Andersen, K.S., Kirkegaard, R.H., Karst, S.M., Albertsen, M., 2018. ampvis2: an R package to analyse and visualise 16S rRNA amplicon data. bioRxiv https://doi.org/10.1101/299537.

Apprill, A., McNally, S., Parsons, R., Weber, L., 2015. Minor revision to V4 region SSU rRNA 806R gene primer greatly increases detection of SAR11 bacterioplankton. Aquat. Microb. Ecol. 75. https://doi.org/10.3354/ame01753.

Åström, E.K.L., Carroll, M.L., Ambrose, W.G.J., Carroll, J., 2016. Arctic cold seeps in marine methane hydrate environments: impacts on shelf macrobenthic community structure offshore Svalbard. Mar. Ecol. Prog. Ser. 552, 1–18. https://doi.org/10.3354/meps11773.

Åström, E.K.L., Carroll, M.L., Ambrose, W.G., Sen, A., Silyakova, A., Carroll, J.L., 2018. Methane cold seeps as biological oases in the high-Arctic deep sea. Limnol. Oceanogr. 63, S209–S231. https://doi.org/10.1002/lno.10732.

Åström, E.K.L., Carroll, M.L., Sen, A., Niemann, H., Ambrose Jr., W.G., Lehmann, M.F., Carroll, J., 2019. Chemosynthesis influences food web and community structure in high-Arctic benthos. Mar. Ecol. Prog. Ser. 629, 19–42. https://doi.org/10.3354/meps13101.

Bernardino, A.F., Levin, L.A., Thurber, A.R., Smith, C.R., 2012. Comparative composition, diversity and trophic ecology of sediment macrofauna at vents, seeps and organic falls. PLoS One 7, e33515. https://doi.org/10.1371/journal.pone.0033515.

Blasco, K.A., Blasco, S.M., Bennett, R., MacLean, B., Rainey, W.A., Davies, E.H., 2010. Seabed geologic features and processes and their relationship with fluid seeps and the benthic environment in the Northwest Passage. Geol. Surv. Canada. Open File 6438, 1–58. https://doi.org/10.4095/287316.

Bodelier, P.L.E., Meima-Franke, M., Hordijk, C.A., Steenbergh, A.K., Hefting, M.M., Bodrossy, L., von Bergen, M., Seifert, J., 2013. Microbial minorities modulate methane consumption through niche partitioning. ISME J. 7, 2214–2228. https://doi.org/10.1038/ismej.2013.99.

Boetius, A., Wenzhöfer, F., 2013. Seafloor oxygen consumption fuelled by methane from cold seeps. Nat. Geosci. 6, 725–734. https://doi.org/10.1038/ngeo1926.

Bouchard Marmen, M., Kenchington, E., Ardyna, M., Archambault, P., 2017. Influence of seabird colonies and other environmental variables on benthic community structure, Lancaster Sound Region, Canadian Arctic. J. Mar. Syst. 167, 105–117. https://doi.org/10.1016/j.jmarsys.2016.11.021.

Capelle, D.W., Dacey, J.W., Tortell, P.D., 2015. An automated, high through-put method for accurate and precise measurements of dissolved nitrous-oxide and methane concentrations in natural waters. Limnol. Oceanogr. Methods 13, 345–355. https://doi.org/10.1002/lom3.10029.

Carney, R.S., 1994. Consideration of the oasis analogy for chemosynthetic communities at Gulf of Mexico hydrocarbon vents. Geo-Marine Lett. 14, 149–159. https://doi.org/10.1007/BF01203726.

Chistoserdova, L., Lidstrom, M.E., 2013. Aerobic methylotrophic prokaryotes. In: Rosenberg, E., DeLong, E.F., Lory, S., Stackebrandt, E., Thompson, F. (Eds.), The Prokaryotes: Prokaryotic Physiology and Biochemistry. Springer, Berlin Heidelberg, Berlin, Heidelberg, pp. 267–285 https://doi.org/10.1007/978-3-642-30141-4_68.

Crépeau, V., Cambon Bonavita, M.A., Lesongeur, F., Randrianalivelo, H., Sarradin, P.M., Sarrazin, J., Godfroy, A., 2011. Diversity and function in microbial mats from the Lucky Strike hydrothermal vent field. FEMS Microbiol. Ecol. 76, 524–540. https://doi.org/10.1111/j.1574-6941.2011.01070.x.

Crespo-Medina, M., Meile, C.D., Hunter, K.S., Diercks, A.R., Asper, V.L., Orphan, V.J., Tavormina, P.L., Nigro, L.M., Battles, J.J., Chanton, J.P., Shiller, A.M., Joung, D.J., Amon, R.M.W., Bracco, A., Montoya, J.P., Villareal, T.A., Wood, A.M., Joye, S.B., 2014. The rise and fall of methanotrophy following a deepwater oil-well blowout. Nat. Geosci. 7, 423–427. https://doi.org/10.1038/ngeo2156.

Dale, J.E., Aitken, A.E., Gilbert, R., Risk, M.J., 1989. Macrofauna of Canadian arctic fjords. Mar. Geol. 85, 331–358. https://doi.org/10.1016/0025-3227(89)90159-X.

Demopoulos, A.W.J., Bourque, J.R., Durkin, A., Cordes, E.E., 2018. The influence of seep habitats on sediment macrofaunal biodiversity and functional traits. Deep. Res. Part I Oceanogr. Res. Pap. 142, 77–93. https://doi.org/10.1016/j.dsr.2018.10.004.

Devine, B.M., Wheeland, L.J., Fisher, J.A.D., 2018. First estimates of Greenland shark (Somniosus microcephalus) local abundances in Arctic waters. Sci. Rep. 8, 974. https://doi.org/10.1038/s41598-017-19115-x.

DFO, 2015. Ecologically and Biologically Significant Areas in Canada's Eastern Arctic Biogeographic Region, 2015. DFO Can. Sci. Advis. Sec. Sci. Advis. Rep. 2015/049.

Dittmar, T., Koch, B., Hertkorn, N., Kattner, G., 2008. A simple and efficient method for the solid-phase extraction of dissolved organic matter (SPE-DOM) from seawater. Limnol. Oceanogr. Methods 6, 230–235. https://doi.org/10.4319/lom.2008.6.230.

Dong, X., Kleiner, M., Sharp, C.E., Thorson, E., Li, C., Liu, D., Strous, M., 2017. Fast and simple analysis of MiSeq amplicon sequencing data with MetaAmp. Front. Microbiol. 8, 1–8. https://doi.org/10.3389/fmicb.2017.01461.

Dumont, M.G., Murrell, J.C., 2005. Community-level analysis: key genes of aerobic methane oxidation. Methods Enzymol. 397, 413–427. https://doi.org/10.1016/S0076-6879(05)97025-0.

Dumont, M.G., Lüke, C., Deng, Y., Frenzel, P., 2014. Classification of pmoA amplicon pyrosequences using BLAST and the lowest common ancestor method in MEGAN. Front. Microbiol. 5, 1–11. https://doi.org/10.3389/fmicb.2014.00034.

Edgar, R.C., 2004. MUSCLE: multiple sequence alignment with high accuracy and high throughput. Nucleic Acids Res. 32, 1792–1797. https://doi.org/10.1093/nar/gkh340.

Edinger, E.N., Sherwood, O.A., Piper, D.J.W., Wareham, V.E., Baker, K.D., Gilkinson, K.D., Scott, D.B., 2011. Geological features supporting deep-sea coral habitat in Atlantic Canada. Cont. Shelf Res. 31, S69–S84. https://doi.org/10.1016/j.csr.2010.07.004.

Elder, C.D., Thompson, D.R., Thorpe, A.K., Walter Anthony, K.M., Miller, C.E., 2020. Airborne mapping reveals emergent power law of arctic methane emissions. Geophys. Res. Lett. 47, e2019GL085707. https://doi.org/10.1029/2019GL085707.

Etminan, M., Myhre, G., Highwood, E.J., Shine, K.P., 2016. Radiative forcing of carbon dioxide, methane, and nitrous oxide: a significant revision of the methane radiative forcing. Geophys. Res. Lett. 43, 12,612–614,623. https://doi.org/10.1002/2016GL071930.

Fenwick, L., Capelle, D., Damm, E., Zimmermann, S., Williams, W.J., Vagle, S., Tortell, P.D., 2017. Methane and nitrous oxide distributions across the North American Arctic Ocean during summer, 2015. J. Geophys. Res. Ocean. 122, 390–412. https://doi.org/10.1002/2016JC012493.

Ferré, B., Jansson, P.G., Moser, M., Serov, P., Portnov, A., Graves, C.A., Panieri, G., Gründger, F., Berndt, C., Lehmann, M.F., Niemann, H., 2020. Reduced methane seepage from Arctic sediments during cold bottom-water conditions. Nat. Geosci. 13, 1–5. https://doi.org/10.1038/s41561-019-0515-3.

Folch, J., Lees, M., Stanley, G.H.S., 1957. A simple method for the isolation and purification of total lipides from animal tissues. J. Biol. Chem. 226, 497–509.

Goffredi, S.K., Tilic, E., Mullin, S.W., Dawson, K.S., Keller, A., Lee, R.W., Wu, F., Levin, L.A., Rouse, G.W., Cordes, E.E., Orphan, V.J., 2020. Methanotrophic bacterial symbionts fuel dense populations of deep-sea feather duster worms (Sabellida, Annelida) and extend the spatial influence of methane seepage. Sci. Adv. 6, eaay8562. https://doi.org/10.1126/sciadv.aay8562.

Grant, A.C., Levy, E.M., Lee, K., Moffat, J.D., 1986. Pisces IV research submersible finds oil on Baffin Shelf. Geol. Surv. Canada, Curr. Res. Part A 86-1A, 65–69.

Hamdan, L.J., Coffin, R.B., Sikaroodi, M., Greinert, J., Treude, T., Gillevet, P.M., 2013. Ocean currents shape the microbiome of Arctic marine sediments. ISME J. 7, 685–696. https://doi.org/10.1038/ismej.2012.143.

Harrison, J.C., Brent, T.A., Oakey, G.N., 2011. Baffin Fan and its inverted rift system of Arctic eastern Canada: stratigraphy, tectonics and petroleum resource potential. Geol. Soc. London. Mem. 35, 595–626. https://doi.org/10.1144/m35.40.

Hovland, M., Risk, M., 2003. Do Norwegian deep-water coral reefs rely on seeping fluids? Mar. Geol. 198, 83–96. https://doi.org/10.1016/S0025-3227(03)00096-3.

Hussey, N.E., Cosandey-Godin, A., Walter, R.P., Hedges, K.J., VanGerwen-Toyne, M., Barkley, A.N., Kessel, S.T., Fisk, A.T., 2015. Juvenile Greenland sharks Somniosus microcephalus (Bloch & Schneider, 1801) in the Canadian Arctic. Polar Biol. 38, 493–504. https://doi.org/10.1007/s00300-014-1610-y.

Jousset, A., Bienhold, C., Chatzinotas, A., Gallien, L., Gobet, A., Kurm, V., Küsel, K., Rillig, M.C., Rivett, D.W., Salles, J.F., van der Heijden, M.G.A., Youssef, N.H., Zhang, X., Wei, Z., Hol, W.H.G., 2017. Where less may be more: how the rare biosphere pulls ecosystems strings. ISME J. 11, 853–862. https://doi.org/10.1038/ismej.2016.174.

van de Kamp, J., Hook, S.E., Williams, A., Tanner, J.E., Bodrossy, L., 2019. Baseline characterization of aerobic hydrocarbon degrading microbial communities in deep-sea sediments of the Great Australian Bight. Australia. Environ. Microbiol. 21, 1782–1797. https://doi.org/10.1111/1462-2920.14559.

Kessler, J.D., Valentine, D.L., Redmond, M.C., Du, M., Chan, E.W., Mendes, S.D., Quiroz, E.W., Villanueva, C.J., Shusta, S.S., Werra, L.M., Yvon-lewis, S.A., Weber, T.C., 2011. A persistent oxygen anomaly reveals the fate of spilled methane in the deep Gulf of Mexico. Science 331, 312–315. https://doi.org/10.1126/science.1199697.

Kilgour, D.P.A., Wills, R., Qi, Y., O'Connor, P.B., 2013. Autophaser: an algorithm for automated generation of absorption mode spectra for FT-ICR MS. Anal. Chem. 85, 3903–3911. https://doi.org/10.1021/ac303289c.

Knief, C., 2015. Diversity and habitat preferences of cultivated and uncultivated aerobic methanotrophic bacteria evaluated based on pmoA as molecular marker. Front. Microbiol. 6. https://doi.org/10.3389/fmicb.2015.01346.

Latour, P.B., Leger, J., Hines, J.E., Mallory, M.L., Mulders, D.L., Gilchrist, H.G., Smith, P.A., Dickson, D.L., 2008. Key migratory bird terrestrial habitat sites in the Northwest Territories and Nunavut. Can. Wildl. Serv. Occas. Pap. 114.

Leonte, M., Kessler, J.D., Kellermann, M.Y., Arrington, E.C., Valentine, D.L., Sylva, S.P., 2017. Rapid rates of aerobic methane oxidation at the feather edge of gas hydrate stability in the waters of Hudson Canyon. US Atlantic Margin. Geochim. Cosmochim. Acta 204, 375–387. https://doi.org/10.1016/j.gca.2017.01.009.

Letunic, I., Bork, P., 2019. Interactive Tree Of Life (iTOL) v4: recent updates and new developments. Nucleic Acids Res. 47, W256–W259. https://doi.org/10.1093/nar/gkz239.

Levin, L.A., Baco, A.R., Bowden, D.A., Colaco, A., Cordes, E.E., Cunha, M.R., Demopoulos, A.W.J., Gobin, J., Grupe, B.M., Le, J., Metaxas, A., Netburn, A.N., Rouse, G.W., Thurber, A.R., Tunnicliffe, V., Van Dover, C.L., Vanreusel, A., Watling, L., 2016. Hydrothermal vents and methane seeps: rethinking the sphere of influence. Front. Mar. Sci. 3, 1–23. https://doi.org/10.3389/fmars.2016.00072.

Levy, E.M., 1978. Visual and chemical evidence for a natural seep at Scott Inlet, Baffin Island, District of Franklin. Geol. Surv. Canada, Curr. Res. Part B 78–1B, 21–26.

Levy, E.M., Lee, K., 1988. Potential contribution of natural hydrocarbon seepage to benthic productivity and the fisheries of Atlantic Canada. Can. J. Fish. Aquat. Sci. 45, 349–352. https://doi.org/10.1139/f88-041.

Levy, E.M., MacLean, B., 1980. Natural hydrocarbon seepage at Scott Inlet and Buchan Gulf, Baffin Island Shelf: 1980 update. Geol. Surv. Canada, Curr. Res. Part A 81-1A, 401–403.

Li, M., Jain, S., Baker, B.J., Taylor, C., Dick, G.J., 2014. Novel hydrocarbon monooxygenase genes in the metatranscriptome of a natural deep-sea hydrocarbon plume. Environ. Microbiol. 16, 60–71. https://doi.org/10.1111/1462-2920.12182.

Loncarevic, B.D., Falconer, R.K., 1977. An oil slick occurrence off Baffin Island. Geol. Surv. Canada 77-1A, 523–524.

Love, M.I., Huber, W., Anders, S., 2014. Moderated estimation of fold change and dispersion for RNA-seq data with DESeq2. Genome Biol. 15, 550. https://doi.org/10.1186/s13059-014-0550-8.

MacAvoy, S.E., Carney, R.S., Fisher, C.R., 2002. Use of chemosynthetic biomass by large, mobile, benthic predators in the Gulf of Mexico. Mar. Ecol. Prog. Ser. 225, 65–78. https://doi.org/10.3354/meps225065.

Maclean, B., Falconer, R.K.H., Levy, E.M., 1981. Geological, geophysical and chemical evidence for natural seepage of petroleum off the northeast coast of Baffin Island. Bull. Can. Petrol. Geol. 29, 75–95.

Mallory, M., Fontaine, A., 2004. Key marine habitat sites for migratory birds in Nunavut and the Northwest Territories. Occas. Pap. Can. Wildl. Serv. 109.
Marcoux, M., Ferguson, S.H., Roy, N., Bedard, J.M., Simard, Y., 2017. Seasonal marine mammal occurrence detected from passive acoustic monitoring in Scott Inlet, Nunavut. Canada. Polar Biol. 40, 1127–1138. https://doi.org/10.1007/s00300-016-2040-9.
Mason, O.U., Han, J., Woyke, T., Jansson, J.K., 2014. Single-cell genomics reveals features of a Colwellia species that was dominant during the Deepwater Horizon oil spill. Front. Microbiol. 5, 332. https://doi.org/10.3389/fmicb.2014.00332.
McDonald, I.R., Bodrossy, L., Chen, Y., Murrell, J.C., 2008. Molecular ecology techniques for the study of aerobic methanotrophs. Appl. Environ. Microbiol. 74, 1305–1315. https://doi.org/10.1128/AEM.02233-07.
Meredyk, S.P., Edinger, E., Piper, D.J.W., Huvenne, V.A.I., Hoy, S., Ruffman, A., 2020. Enigmatic deep-water mounds on the orphan knoll, Labrador Sea. Front. Mar. Sci. 6, 744. https://doi.org/10.3389/fmars.2019.00744.
Mort, A., Currie, L., Haggart, J., Osadetz, K., 2013. Geochemical investigation of undiscovered petroleum systems in Baffin Bay, eastern Canada. In: González-Pérez, J.A., González-Vila, F.L., Jiménez-Morillo, N.T., Almendros, G. (Eds.), 26th International Meeting on Organic Geochemistry, Organic Geochemistry: Trends for the 21st Century. Book of Abstracts, European Association of Organic Geochemists, pp. 408–409.
Neufeld, J.D., Chen, Y., Dumont, M.G., Murrell, J.C., 2008. Marine methylotrophs revealed by stable-isotope probing, multiple displacement amplification and metagenomics. Environ. Microbiol. 10, 1526–1535. https://doi.org/10.1111/j.1462-2920.2008.01568.x.
Neves, B.M., Du Preez, C., Edinger, E., 2014. Mapping coral and sponge habitats on a shelf-depth environment using multibeam sonar and ROV video observations: Learmonth Bank, northern British Columbia, Canada. Deep Sea Res. Part II Top. Stud. Oceanogr. 99, 169–183. https://doi.org/10.1016/j.dsr2.2013.05.026.
Niemann, H., Linke, P., Knittel, K., MacPherson, E., Boetius, A., Brückmann, W., Larvik, G., Wallmann, K., Schacht, U., Omoregie, E., Hilton, D., Brown, K., Rehder, G., 2013. Methane-carbon flow into the benthic food web at cold seeps - a case study from the Costa Rica subduction zone. PLoS One 8, 4–13. https://doi.org/10.1371/journal.pone.0074894.
Oldenburg, T.B.P., Brown, M., Bennett, B., Larter, S.R., 2014. The impact of thermal maturity level on the composition of crude oils, assessed using ultra-high resolution mass spectrometry. Org. Geochem. 75, 151–168. https://doi.org/10.1016/J.ORGGEOCHEM.2014.07.002.
Oldenburg, T.B.P., Jones, M., Huang, H., Bennett, B., Shafiee, N.S., Head, I., Larter, S.R., 2017. The controls on the composition of biodegraded oils in the deep subsurface – part 4. Destruction and production of high molecular weight non-hydrocarbon species and destruction of aromatic hydrocarbons during progressive in-reservoir biodegradation. Org. Geochem. 114, 57–80. https://doi.org/10.1016/J.ORGGEOCHEM.2017.09.003.
Parada, A.E., Needham, D.M., Fuhrman, J.A., 2016. Every base matters: assessing small subunit rRNA primers for marine microbiomes with mock communities, time series and global field samples. Environ. Microbiol. 18, 1403–1414. https://doi.org/10.1111/1462-2920.13023.
Parmentier, F.J.W., Christensen, T.R., Sørensen, L.L., Rysgaard, S., Mcguire, A.D., Miller, P.A., Walker, D.A., 2013. The impact of lower sea-ice extent on Arctic greenhouse-gas exchange. Nat. Clim. Chang. 3, 195–202. https://doi.org/10.1038/nclimate1784.
Parrish, C.C., 1999. Determination of total lipid, lipid classes, and fatty acids in aquatic samples. In: Arts, M.T., Wainman, B.C. (Eds.), Lipids in Freshwater Ecosystems. Springer New York, New York, NY, pp. 4–20 https://doi.org/10.1007/978-1-4612-0547-0_2.
Pop Ristova, P., Wenzhöfer, F., Ramette, A., Felden, J., Boetius, A., 2015. Spatial scales of bacterial community diversity at cold seeps (Eastern Mediterranean Sea). ISME J. 9, 1306–1318. https://doi.org/10.1038/ismej.2014.217.
Price, M.N., Dehal, P.S., Arkin, A.P., 2009. FastTree: computing large minimum evolution trees with profiles instead of a distance matrix. Mol. Biol. Evol. 26, 1641–1650. https://doi.org/10.1093/molbev/msp077.
Pruesse, E., Peplies, J., Glöckner, F.O., 2012. SINA: accurate high-throughput multiple sequence alignment of ribosomal RNA genes. Bioinformatics 28, 1823–1829. https://doi.org/10.1093/bioinformatics/bts252.
Punshon, S., Azetsu-Scott, K., Sherwood, O., Edinger, E.N., 2019. Bottom water methane sources along the high latitude eastern Canadian continental shelf and their effects on the marine carbonate system. Mar. Chem. 212, 83–95. https://doi.org/10.1016/j.marchem.2019.04.004.
R Core Team, 2019. R: A Language and Environment for Statistical Computing.
Redmond, M.C., Valentine, D.L., 2012. Natural gas and temperature structured a microbial community response to the Deepwater Horizon oil spill. Proc. Natl. Acad. Sci. 109, 20292–20297. https://doi.org/10.1073/pnas.1108756108.
Reeburgh, W.S., 2007. Oceanic methane biogeochemistry. Chem. Rev. 107, 486–513. https://doi.org/10.1021/cr050362v.
Roy, V., Iken, K., Archambault, P., 2014. Environmental drivers of the Canadian Arctic megabenthic communities. PLoS One 9, e100900. https://doi.org/10.1371/journal.pone.0100900 19 pages.
Ruff, S.E., Hrabe de Angelis, I., 2019. VisuaR: An R-Based Workflow for the Analysis and Visualization of Sequence Data (GitHub).
Ruff, S.E., Biddle, J.F., Teske, A.P., Knittel, K., Boetius, A., Ramette, A., 2015. Global dispersion and local diversification of the methane seep microbiome. Proc. Natl. Acad. Sci. 112, 4015–4020. https://doi.org/10.1073/pnas.1421865112.
Sahling, H., Galkin, S.V., Salyuk, A., Greinert, J., Foerstel, H., Piepenburg, D., Suess, E., 2003. Depth-related structure and ecological significance of cold-seep communities—a case study from the Sea of Okhotsk. Deep Sea Res. Part I Oceanogr. Res. Pap. 50, 1391–1409. https://doi.org/10.1016/j.dsr.2003.08.004.
Salvo, F., Hamoutene, D., Hayes, V.E.W., Edinger, E.N., Parrish, C.C., 2018. Investigation of trophic ecology in Newfoundland cold-water deep-sea corals using lipid class and fatty acid analyses. Coral Reefs 37, 157–171. https://doi.org/10.1007/s00338-017-1644-z.
Schloss, P.D., Westcott, S.L., Ryabin, T., Hall, J.R., Hartmann, M., Hollister, E.B., Lesniewski, R.A., Oakley, B.B., Parks, D.H., Robinson, C.J., Sahl, J.W., Stres, B., Thallinger, G.G., Van Horn, D.J., Weber, C.F., 2009. Introducing mothur: open-source, platform-independent, community-supported software for describing and comparing microbial communities. Appl. Environ. Microbiol. 75, 7537–7541. https://doi.org/10.1128/AEM.01541-09.
Schneider, C.A., Rasband, W.S., Eliceiri, K.W., 2012. NIH image to ImageJ: 25 years of image analysis. Nat. Methods 9, 671–675. https://doi.org/10.1038/nmeth.2089.
Seabrook, S., De Leo, C., Baumberger, T., Raineault, N., Thurber, A.R., 2018. Heterogeneity of methane seep biomes in the Northeast Pacific. Deep. Res. Part II Top. Stud. Oceanogr. 150, 195–209. https://doi.org/10.1016/j.dsr2.2017.10.016.
Seabrook, S., De Leo, F.C., Thurber, A.R., 2019. Flipping for food: the use of a methane seep by tanner crabs (Chionoecetes tanneri). Front. Mar. Sci. 6, 1–11. https://doi.org/10.3389/fmars.2019.00043.
Sen, A., Åström, E.K.L., Hong, W.L., Portnov, A., Waage, M., Serov, P., Carroll, M.L., Carroll, J., 2018. Geophysical and geochemical controls on the megafaunal community of a high Arctic cold seep. Biogeosciences 15, 4533–4559. https://doi.org/10.5194/bg-15-4533-2018.
Serreze, M.C., Barry, R.G., 2011. Processes and impacts of Arctic amplification: a research synthesis. Glob. Planet. Change 77, 85–96. https://doi.org/10.1016/j.gloplacha.2011.03.004.
Shakhova, N., Semiletov, I., Salyuk, A., Yusupov, V., Kosmach, D., Gustafsson, O., 2010. Extensive methane venting to the atmosphere from sediments of the East Siberian Arctic Shelf. Science 327, 1246–1250. https://doi.org/10.1126/science.1182221.
Silva, R.C., Radović, J.R., Ahmed, F., Ehrmann, U., Brown, M., Carbognani Ortega, L., Larter, S., Pereira-Almao, P., Oldenburg, T.B.P., 2016. Characterization of acid-soluble oxidized asphaltenes by Fourier transform ion cyclotron resonance mass spectrometry: insights on oxycracking processes and asphaltene structural features. Energy Fuel 30, 171–179. https://doi.org/10.1021/acs.energyfuels.5b02215.
Silyakova, A., Jansson, P., Serov, P., Ferré, B., Pavlov, A.K., Hattermann, T., Graves, C.A., Platt, S.M., Myhre, C.L., Gründger, F., Niemann, H., 2020. Physical controls of dynamics of methane venting from a shallow seep area west of Svalbard. Cont. Shelf Res. 194, 104030. https://doi.org/10.1016/j.csr.2019.104030.
Suess, E., 2014. Marine cold seeps and their manifestations: geological control, biogeochemical criteria and environmental conditions. Int. J. Earth Sci. 103, 1889–1916. https://doi.org/10.1007/s00531-014-1010-0.
Suess, E., 2018. Marine cold seeps: background and recent advances. Hydrocarb. Oils Lipids Divers. Orig. Chem. Fate, 1–21 https://doi.org/10.1007/978-3-319-54529-5_27-1.
Tavormina, P.L., Ussier, W., Orphan, V.J., 2008. Planktonic and sediment-associated aerobic methanotrophs in two seep systems along the North American margin. Appl. Environ. Microbiol. 74, 3985–3995. https://doi.org/10.1128/AEM.00069-08.
Tavormina, P.L., Hatzenpichler, R., McGlynn, S., Chadwick, G., Dawson, K.S., Connon, S.A., Orphan, V.J., 2015. Methyloprofundus sedimenti gen. nov., sp. nov., an obligate methanotroph from ocean sediment belonging to the 'deep sea-1' clade of marine methanotrophs. Int. J. Syst. Evol. Microbiol. 65, 251–259. https://doi.org/10.1099/ijs.0.062927-0.
Teske, A., Carvalho, V., 2020. Large sulfur-oxidizing bacteria at Gulf of Mexico hydrocarbon seeps. In: Teske, A.P., Carvalho, V. (Eds.), Marine Hydrocarbon Seeps. Springer Oceanography, Switzerland, pp. 149–171.
Thornton, B.F., Crill, P., 2015. Arctic permafrost: microbial lid on subsea methane. Nat. Clim. Chang. 5, 723–724. https://doi.org/10.1038/nclimate2740.
Thurber, A.R., Kröger, K., Neira, C., Wiklund, H., Levin, L.A., 2010. Stable isotope signatures and methane use by New Zealand cold seep benthos. Mar. Geol. 272, 260–269. https://doi.org/10.1016/j.margeo.2009.06.001.
Thurber, A.R., Levin, L.A., Rowden, A.A., Sommer, S., Linke, P., Kröger, K., 2013. Microbes, macrofauna, and methane: a novel seep community fueled by aerobic methanotrophy. Limnol. Oceanogr. 58, 1640–1656. https://doi.org/10.4319/lo.2013.58.5.1640.
Thurber, A.R., Seabrook, S., Welsh, R.M., 2020. Riddles in the cold: Antarctic endemism and microbial succession impact methane cycling in the Southern Ocean. Proc. R. Soc. B Biol. Sci. 287, 20201134. https://doi.org/10.1098/rspb.2020.1134.
Tremblay, J., Fortin, N., Elias, M., Wasserscheid, J., King, T.L., Lee, K., Greer, C.W., 2019. Metagenomic and metatranscriptomic responses of natural oil degrading bacteria in the presence of dispersants. Environ. Microbiol. 21, 2307–2319. https://doi.org/10.1111/1462-2920.14609.
Valentine, D.L., 2011. Emerging topics in marine methane biogeochemistry. Annu. Rev. Mar. Sci. 3, 147–171. https://doi.org/10.1146/annurev-marine-120709-142734.
Vanreusel, A., Anderson, A., Boetius, A., Connelly, D., Cunha, M.R., Decker, C., Hilario, A., Kormas, K.A., Maignien, L., Olu, K., Pachiadaki, M., Ritt, B., Rodrigues, C., Sarrazin, J., Tyler, P., Van Gaever, S., Vanneste, H., 2009. Biodiversity of cold seep ecosystems along the European margins. Oceanography 22, 110–127.
Voight, J.R., 2000. A deep-sea octopus (Graneledone cf. boreopacifica) as a shell-crushing hydrothermal vent predator. J. Zool. 252, 335–341. https://doi.org/10.1111/j.1469-7998.2000.tb00628.x.
Walsh, E.A., Kirkpatrick, J.B., Rutherford, S.D., Smith, D.C., Sogin, M., D'Hondt, S., 2016. Bacterial diversity and community composition from seasurface to subseafloor. ISME J. 10, 979–989. https://doi.org/10.1038/ismej.2015.175.
Webb, K.E., Barnes, D.K.A., Plankea, S., 2009. Pockmarks: refuges for marine benthic biodiversity. Limnol. Oceanogr. 54, 1776–1788. https://doi.org/10.4319/lo.2009.54.5.1776.
Wen, X., Yang, S., Liebner, S., 2016. Evaluation and update of cutoff values for methanotrophic pmoA gene sequences. Arch. Microbiol. 198, 629–636. https://doi.org/10.1007/s00203-016-1222-8.
Wilson, S.T., Bange, H.W., Arévalo-Martínez, D.L., Barnes, J., Borges, A.V., Brown, I., Bullister, J.L., Burgos, M., Capelle, D.W., Casso, M., De La Paz, M., Farías, L., Fenwick, L., Ferrón, S., Garcia, G., Glockzin, M., Karl, D.M., Kock, A., Laperriere, S., Law, C.S., Manning, C.C., Marriner, A., Myllykangas, J.P., Pohlman, J.W., Rees, A.P., Santoro, A.E., Tortell, P.D., Upstill-Goddard, R.C., Wisegarver, D.P., Zhang, G.L., Rehder, G., 2018.

An intercomparison of oceanic methane and nitrous oxide measurements. Biogeosciences 15, 5891–5907. https://doi.org/10.5194/bg-15-5891-2018.
Yang, S., Wen, X., Liebner, S., 2016. pmoA gene reference database (fasta-formatted sequences and taxonomy). https://doi.org/10.5880/GFZ.5.3.2016.001.
Yvon-Lewis, S.A., Hu, L., Kessler, J., 2011. Methane flux to the atmosphere from the Deepwater horizon oil disaster. Geophys. Res. Lett. 38, 1–5. https://doi.org/10.1029/2010GL045928.
Zbinden, M., Shillito, B., Le Bris, N., de Villardi de Montlaur, C., Roussel, E., Guyot, F., Gaill, F., Cambon-Bonavita, M.-A., 2008. New insigths on the metabolic diversity among the epibiotic microbial communitiy of the hydrothermal shrimp Rimicaris exoculata. J. Exp. Mar. Bio. Ecol. 359, 131–140. https://doi.org/10.1016/j.jembe.2008.03.009.
Zhang, Z., Schwartz, S., Wagner, L., Miller, W., 2000. A greedy algorithm for aligning DNA sequences. J. Comput. Biol. 7, 203–214. https://doi.org/10.1089/10665270050081478.